Integration of multi-omics and deep phenotyping provides novel insights into multiple abiotic stress responses in potato

Maja Zagorščak[1]*, Lamis Abdelhakim[2]*, Natalia Yaneth Rodriguez-Granados[3]*, Jitka Široká[4]*, Arindam Ghatak[5]*, Carissa Bleker[1], Andrej Blejec[1], Jan Zrimec[1], Ondřej Novák[4], Aleš Pěnčík[4], Špela Baebler[1], Lucia Perez Borroto[6], Christian Schuy[7], Anže Županič[1], Leila Afjehi-Sadat[8], Bernhard Wurzinger[5], Wolfram Weckwerth[5,9], Maruša Pompe Novak[1,10], Marc R. Knight[11], Miroslav Strnad[4], Christian Bachem[6], Palak Chaturvedi[5], Sophia Sonnewald[7+], Rashmi Sasidharan[3+], Klára Panzarová[2+], Kristina Gruden[1+#], Markus Teige[5+#]

Affiliations:
[1] Department of Biotechnology and Systems Biology, National Institute of Biology, Večna pot 121, 1000 Ljubljana, Slovenia
[2] PSI (Photon Systems Instruments), spol. s r.o., Prumyslova 470, CZ-664 24 Drásov, Czech Republic
[3] Plant Stress Resilience, Institute of Environmental Biology, Utrecht University, Heidelberglaan 8, 3584 CS Utrecht, The Netherlands
[4] Laboratory of Growth Regulators, Palacký University in Olomouc & Institute of Experimental Botany AS CR, Šlechtitelů 27, Olomouc, 779 00, Czech Republic
[5] Molecular Systems Biology (MOSYS), Department of Functional and Evolutionary Ecology, University Vienna, Djerassiplatz 1, 1030 Vienna, Austria
[6] Wageningen University and Research, Plant Breeding, Droevendaalsesteeg 1, 6708 PB Wageningen, The Netherlands
[7] Department Biologie, Lehrstuhl für Biochemie, Friedrich-Alexander-Universität Erlangen-Nürnberg, Staudstr. 5, 91058 Erlangen, Germany
[8] Mass Spectrometry unit, Research Support Facilities, Faculty of Life Sciences, University Vienna, Djerassiplatz 1, 1030 Vienna, Austria
[9] Vienna Metabolomics Center (VIME), University Vienna, Djerassiplatz 1, 1030 Vienna, Austria
[10] School for Viticulture and Enology, University of Nova Gorica, Gladni trg 8, 5271 Vipava, Slovenia
[11] Department of Biosciences, Durham University, South Road, Durham DH1 3LE, United Kingdom

* shared first authorship
+ shared last authorship
# corresponding authors

Keywords: potato, *Solanum tuberosum*, abiotic stress responses, heat, drought, waterlogging, multi-omics, integrative omics, adaptomics, panomics

Abstract

Potato, the most important non-cereal crop, is highly water and space efficient but susceptible to abiotic stress such as heat, drought, or flooding. Climate change is severely increasing the likelihood of such stresses to occur individually, sequentially, or simultaneously. However, the understanding of acclimation to abiotic stress in crops in general, especially with multiple stresses, is still very limited. Here, we present a comprehensive one month-long molecular and physiological high-throughput profiling of potato (*Solanum tuberosum*, cv. Désirée) under both single and multiple abiotic stresses, designed to mimic realistic future scenarios. Acclimation time-responses were monitored via daily phenomic analysis and leaf samples were processed for multi-omics spanning from transcriptomics to proteomics and hormonomics. Additionally, critical metabolites of tuber samples were analysed at the end of the period. To facilitate the multi-omics analyses, the dataset was integrated with prior knowledge, which is indispensable for development of high-throughput pipelines in agricultural research. Waterlogging had the most immediate and dramatic effects, with responses similar to drought stress. In addition, we observed distinct stress signatures at multiple molecular levels in response to heat or drought and to a combination of both. In general, there was a downregulation of photosynthesis at different molecular levels, accumulation of minor amino acids and diverse stress induced hormones. Our integrative multi-omics analysis provides global insights into plant stress responses, facilitating improved breeding strategies.

One Sentence Summary

Integrated multi-omics analysis of high-throughput phenotyping in potato reveals distinct molecular signatures of acclimation to single and combined abiotic stresses related to climate change.

INTRODUCTION

Improving crop resilience to climate change is a major challenge of modern agriculture (Bailey-Serres et al., 2019; Rivero et al., 2022). Most high-yielding crop varieties are vulnerable to heat, drought, and flooding (Benitez-Alfonso et al., 2023; Zandalinas et al., 2023; Renziehausen et al., 2024; Sato et al., 2024). Global warming has increased the occurrence of such extreme weather events, and thus poses a considerable threat to crop productivity worldwide (FAO, 2023). To ensure future food security, there is an urgent need for sustainable farming practices including the development of stress tolerant varieties with consistent yields.

Mostly from studies performed in model plants, we know that abiotic stress has profound effects on plant metabolism and development. The primary effects of abiotic stress are generation of reactive oxygen species (ROS), destabilisation of proteins and protein complexes, reduction of enzyme efficiencies and alteration of membrane fluidity and integrity (Zhang et al., 2022). Together, these impacts reduce productivity through changes in photosynthetic capacity, hormone balance, transport of assimilates from source to sink as well as transport of soil nutrients and water by the roots. In addition, plants have species-specific vulnerabilities that impact agronomic productivity. In potato (*Solanum tuberosum*) this relates to tuber initiation, and tuber growth dynamics.

Potato is the most consumed non-cereal crop worldwide, cultivated in 150 countries across 18.4 million ha globally (George et al., 2017). After its domestication in the South American Andes about 8000 years ago, potato has become a staple food crop due to its water-use efficiency and contribution to dietary energy intake (Tang et al., 2022). Despite extensive cultivation and over 150 years of breeding, potato remains highly vulnerable to a diverse array of abiotic stresses (Dahal et al., 2019), such as high temperatures and water extremes. These environmental stresses affect plant growth, source-sink relationships, sugar and hormone metabolism, among other processes, which in turn, negatively impact tuber yield and nutritional status (Lal et al., 2022). These adverse climatic conditions require novel approaches to develop crops with increased stress resilience, which is in high demand from farmers (von Gehren et al., 2023).

Potato tuber formation and growth depend on tuberisation signals produced in source leaves, such as the mobile tuberigen StSP6A (Navarro et al., 2011) that also regulates directional transport of sucrose to the developing tuber (Abelenda et al., 2019). StSP6A expression is regulated by day-length and the circadian clock (Kloosterman et al., 2013). Heat, drought and

flooding trigger strong changes in gene expression and thereby strongly interfere with the regulation of flowering and tuberisation by the photoperiodic pathway. This leads to a delay in tuberisation and anomalies in subsequent tuber development such as second-growth and/or internal defects which together severely impact marketable yields of the tuber crop.

There is already a good understanding of how plants react to single abiotic stresses. However, the response of plants to combined stresses is unique and cannot be extrapolated from the response to the corresponding individual stresses, which has been known for almost 20 years (Mittler, 2006). Considering the increasing occurrences of simultaneous or sequential abiotic stresses in the field, the relative lack of knowledge on multi-stress resilience is a major shortfall that hinders the ability to develop effective strategies for crop improvement. Accordingly, the question of how combinations of different stresses, also called multifactorial stress combination (MFSC), impact plants gained a lot of interest (Zandalinas et al., 2021). A number of studies on effects of combinatorial stress in crop plants were recently published, for example, Demirel et al. studied physiological and molecular responses to combined heat- and drought stress in potato (Demirel et al., 2020); Manjunath et al. studied responses to combined heat- and drought stress in wheat (Manjunath et al., 2023); Sinha et al. reported effects of combined low-level abiotic stresses in rice and maize (Sinha et al., 2024); and Zeng et al. studied combined effects of heat- and drought stress on carbon assimilation in tomato (Zeng et al., 2024).

In nature, heat and drought often occur together, resulting in different physiological responses as compared to individual stresses. For example, under heat stomatal conductance and transpiration are increased to reduce leaf temperature, while under drought stomata are closed to avoid water loss, which leads to a strongly reduced CO_2-assimilation (Zhang and Sonnewald, 2017). The final phenotypic output in a combined stress scenario greatly depends on synergistic and antagonistic interactions between stress-specific signalling and response pathways. Furthermore, these interactions can be regulated at various levels (gene expression to metabolism), and on different scales (cell to system), thus resulting in complex regulatory network perturbations. Thus, determining the response in a multi-stress situation is becoming crucial because information gained by extrapolating from studies on individual stressors is limited.

Potato is particularly sensitive to waterlogging (Jovović et al., 2021) and flooding of the fields can ruin the entire harvest within a few days. Due to climate change, yield losses due to waterlogging will dramatically increase in the coming years (Liu et al., 2023). Despite this, little is known about

the molecular mechanisms underlying this vulnerability. Similarly, knowledge about pivotal regulators and gene targets of multi- stress responses and resilience is lacking. Studying holistic multi-stress responses can therefore accelerate target gene discovery and counterbalance the slow progress in potato genetic gain due to the time-consuming and cumbersome breeding process. In particular, genetic improvement of potato is hampered by the complex genetics of this autotetraploid, highly heterozygous crop species. Its genetic load results in severe inbreeding depression when self-fertilized, leading to extremely long breeding cycles (15-25 years) to introduce new traits from wild accessions (Bradshaw et al., 2008).

Rapid technological innovations in the post-omics era have enabled studies examining molecular mechanisms at multiple levels and in multiple processes simultaneously. The combination of high-throughput phenotyping platforms and integrative omics technologies is an innovative and holistic approach to obtain a comprehensive understanding of the intricate dynamics of plant-environment interactions (Yang et al., 2020; Hall et al., 2022; Zhang et al., 2022). This will guide the development of diagnostic markers for rapid detection of stress allowing for earlier interventions in agricultural practice to enhance plant resilience towards abiotic stress. Ultimately, such markers can be further developed in panomics approaches to aid novel marker-assisted breeding programs for climate-resilient crops (Weckwerth et al., 2020; Mishra et al., 2024).

In this study, we carried out a comprehensive assessment of potato responses to single and combined heat, drought, and waterlogging stress. Using the cv. Désirée, a widely used moderate stress-resistant potato cultivar, we monitored dynamic changes in morphological, physiological as well as biochemical and molecular responses under stress conditions. With the application of high throughput phenotyping, multi-omics technologies, prior-knowledge and multi-level integration approaches, we identified important molecular signatures unique to single and different stress combinations.

The huge amount of data resulting from this multi-omics analysis required the development of a novel data integration pipeline to systematically extract the biological meaning of the large data sets in an unbiased way. In plant sciences this is urgently needed because in contrast to the medical field, only a few publications addressed the problem of data integration from comprehensive multi-omics studies (Jamil et al., 2020). The increasing application of high-throughput approaches in agricultural research makes this challenge even more pressing. The integrative approach developed here leveraged statistics, machine learning, and graph theory,

and enabled molecular insights across various system levels, enhanced target prediction and disentangled the intricate physiological and molecular crosstalk, particularly in the context of non-additive effects of different stress combinations.

RESULTS

High throughput physiological phenotyping of potato in multi-stress conditions

This study aims to increase understanding of crop acclimation to abiotic stresses by focusing on most likely scenarios for future agriculture: individual heat, drought and waterlogging stress, and realistic combinations thereof. We studied the cv. Désirée, a widely used moderately stress-resistant potato cultivar, as a model. Daily phenotyping using image-based sensors and regular sampling of leaf material for downstream molecular and biochemical analysis allowed better insights into the mechanisms of the stress response. Single and combined stresses were applied to 4-week-old plants during the tuber initiation stage according to the scheme in Figure 1A (for more details see Supp. Table 1). Daily phenotyping of plants under control and stress conditions was performed using the PlantScreen^{TM} phenotyping platform to assess quantitative morphological and physiological traits, employing multiple imaging sensors (Figure 1B, Supp. Table 2, Supp. Table 5). Plants were light adapted before chlorophyll fluorescence measurements to ensure steady conditions prior to the measurements.

Effects of single and combined stresses on potato growth and morphology

By using RGB side and top view imaging, we monitored plant growth dynamics, including traits such as plant volume, area, height and compactness. We showed that the exponential growth of plants observed under control conditions was negatively impacted to various extent by different stresses (Figure 1C, Supp. Figure 1). Under heat stress (H, 30°C during day, 28°C during night) the rate of biomass accumulation (plant volume) was decreased after three days similarly to drought stress (D, 30% of max. soil water capacity) (Figure 1C, Supp. Figure 1A-C). Distinct morpho-physiological alterations became visible in response to heat and waterlogging. Heat clearly reduced plant height and caused the typical hyponastic growth of leaves (Figure 1A and Supp Figure 1C). The negative effects of heat became more severe when combined with drought (HD, water withdrawal starting after 7 days of H) (Supp Figure 1C).

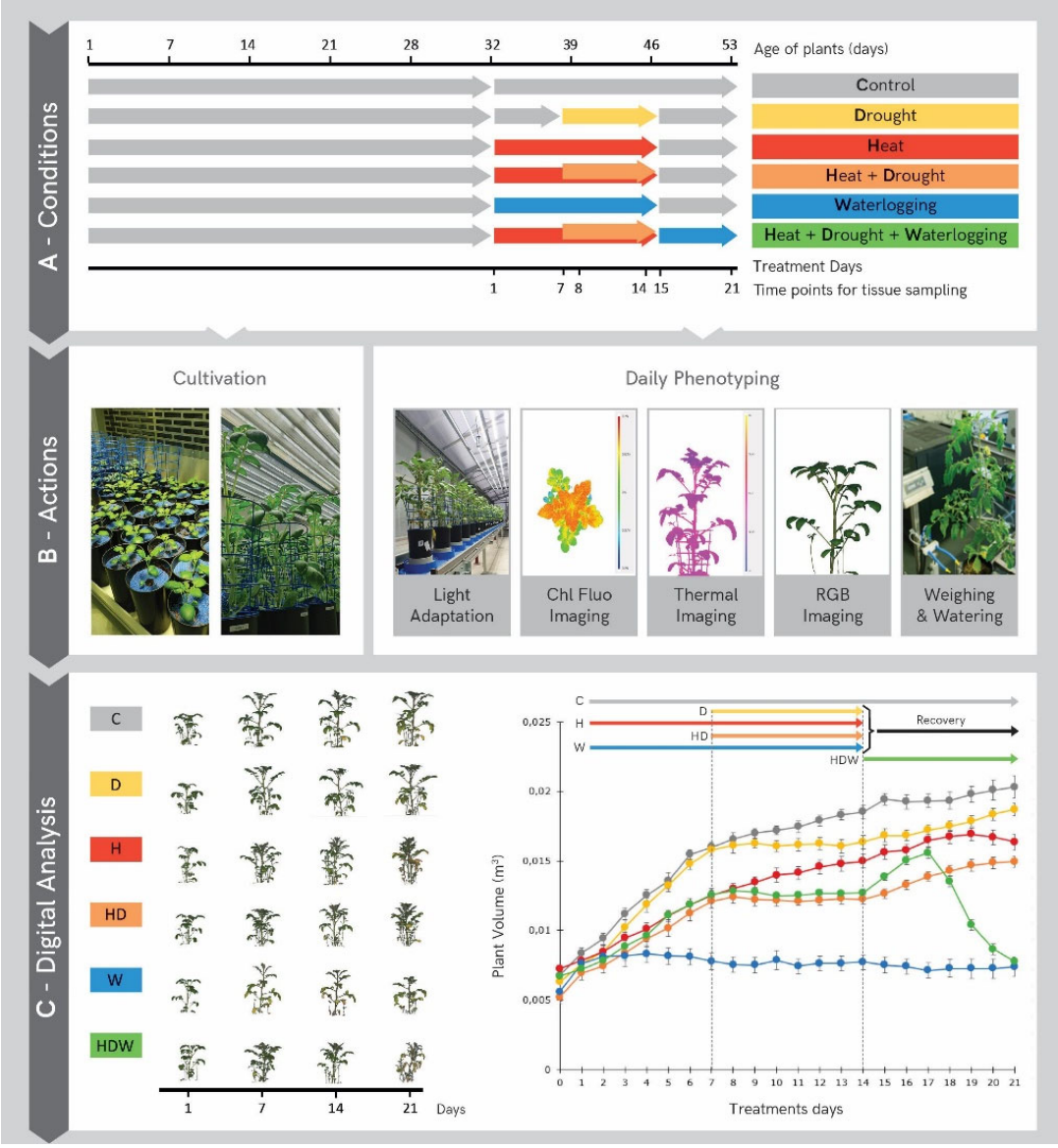

Figure 1. Overview of the experimental design for single- and combined stress treatments and multi-omics sampling. A) Summary of cultivation conditions. Timeline of the experimental set-up and applied stress treatments, including the recovery phase in potato cv. Désirée. Timing and duration of stress treatment and days for tissue sampling are shown. (B) Actions comprised cultivation in the growing chambers and daily phenotyping with a set of sensors using the PlantScreen™ phenotyping platform at PSI Research Center. (C) Automated image analysis pipeline was used to extract quantitative traits for morphological, physiological, and biochemical performance characterization of the plants during the stress treatment and recovery phase. Side view colour segmented RGB images of plants at selected time points of tissue sampling (left panel) and daily plant volume (m^3) calculated from top and multiple angle side view RGB images (right panel). N=6.

Under HD combination, plants phenotypically more resembled heat-stressed plants, e.g. with respect to top area and compactness, however, with a clearly more negative effect (Supp. Figure 1B, 1D). Waterlogging led to an epinastic leaf movement which was accompanied by growth arrest and a significant decrease in top area, compactness and relative growth rate (RGR) that were observed already within first 24h (Figure 1C, Supp. Figure 1A, 1B, 1D, 1E). In the 3rd week, when the single and HD stress treatments were finished (at treatment day 15), plants recovered well from H and HD, but not from W stress, which was clearly reflected by resumption of growth (Figure 1C, Supp. Figure 1B).

Plant performance was the worst in the triple-stress condition (HDW), where 7 days of H were followed by 7 days of combined HD and 7 days of waterlogging. Interestingly, during the first three days of waterlogging that followed the period of heat and drought plants were growing very fast, but with prolonged exposure plants collapsed, as indicated from the RGB side and top view images as well as plant volume as an indicator for growth and RGR (Figure 1C, Supp. Figure 1A, 1E).

Photosynthesis is most affected by heat- and drought stress

To find traits of interest and evaluate photosynthetic performance under single and multiple stresses, a broad range of physiological traits were extracted and analysed (Figure 2). Chlorophyll fluorescence images clearly showed the impact of stress reflected by the reduction of the QY_Lss (operating efficiency of photosystem II in light) (Figure 2A, 2B). Both F_v/F_m_Lss (steady-state fluorescence of maximum efficiency of PSII in the light) and qL_Lss (steady-state estimation of the fraction of open reaction centers in PSII in the light) showed a significant reduction in W and HDW conditions (Figure 2C, 2D). H also resulted in a reduced QY_Lss (Figure 2A, 2B). Furthermore, a decrease in qL_Lss was observed already after one day of H and remained constantly lower than in other conditions, while D caused no significant effect on these parameters Figure 2D). By applying drought in addition to heat stress, an increase in qL_Lss as compared to H alone was observed. Photosynthesis-related traits including the F_v/F_m_Lss and qL_Lss were improved after H and HD recovery, but still did not reach control levels at the end of the experiment by day 21 (Figure 2C and 2D), suggesting that photosynthesis is enduringly affected. In contrast, in W and HDW both parameters decrease even further after recovery, indicating a high stress level.

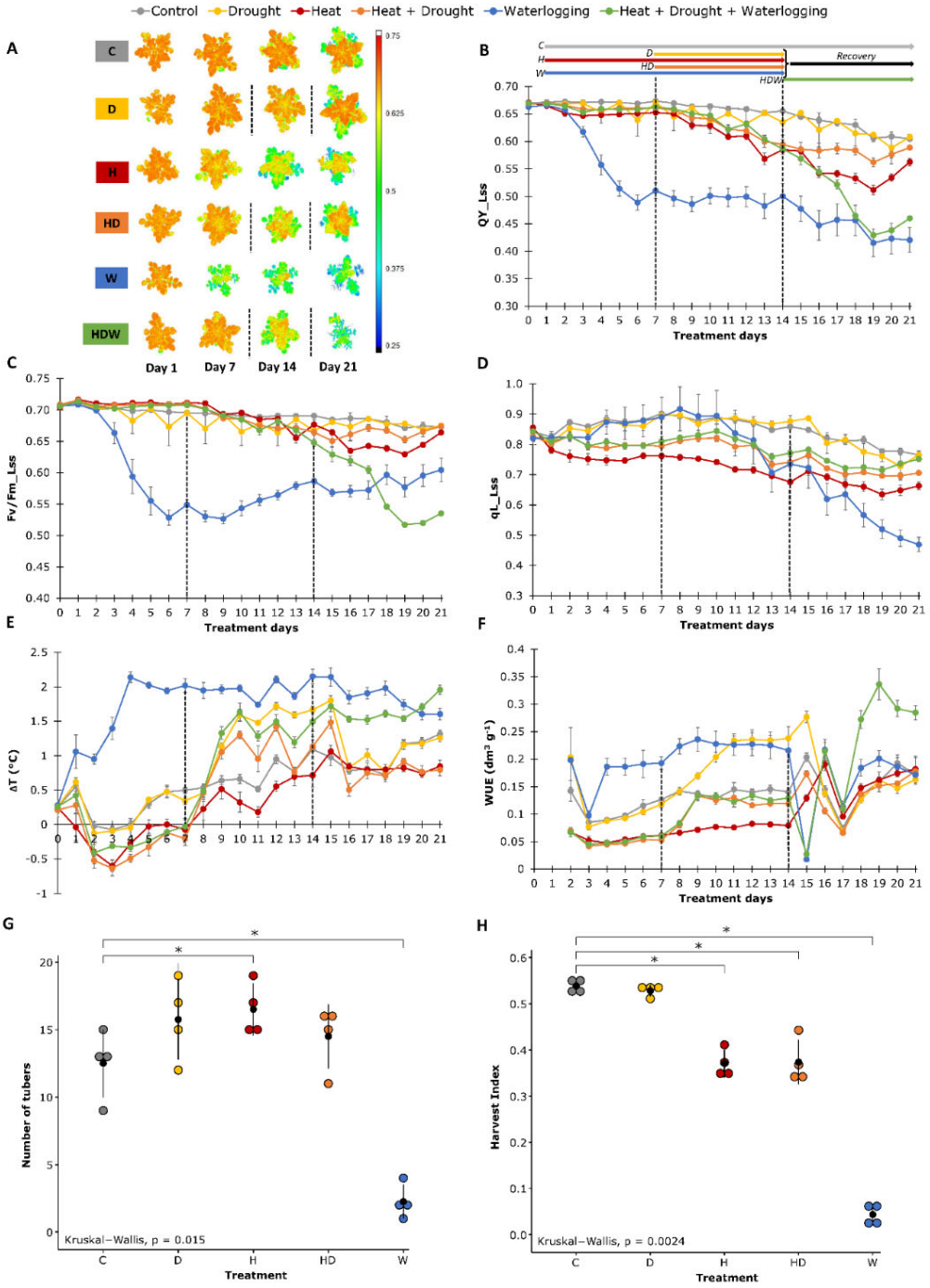

Figure 2. Physiological profiling using high-throughput phenotyping platforms reveals distinct responses to single and combined stresses. A) Pixel-by-pixel false colour images of operating efficiency of photosystem II in light steady state (QY_Lss) captured by kinetic chlorophyll fluorescence measurement. Images for selected time points of tissue sampling are shown. Colour coding of the treatments apply for the entire figure. Vertical dashed lines indicate the onset and end of drought. B) QY_Lss values extracted from

images for each individual time point. C) Steady-state fluorescence of maximum efficiency of PSII photochemistry in the light trait based on chlorophyll fluorescence top view (F_v/F_m_Lss). D) steady-state estimation of the fraction of open reaction centers in PSII trait in light based on chlorophyll fluorescence top view (qL_Lss). E) Difference between canopy average temperature extracted from thermal IR images and air temperature measured in the thermal IR imaging unit (ΔT). F) Water use efficiency (WUE) based on plant volume and water consumption. A-F) Black dotted lines reflect the initiation and removal of drought stress, respectively. G) Tuber numbers counted per plant on the last day of the experiment (Day 28 = 60 days of cultivation). H) Harvest index calculated from the total biomass and tuber weight on the last day of the experiment. G-H) Measurements, mean and standard deviation are shown (n = 4). Statistical evaluation of differences between groups is given by the non-parametric Kruskal–Wallis test (*one-way ANOVA on ranks*); p-value above x-axis, where asterisk denotes p-value < 0.05. See Figure 1A for scheme of stress treatments.

In addition, changes in canopy temperature (ΔT) were deduced from the thermal imaging, and water use efficiency (WUE) that was calculated based on water consumption. The rapid increase in ΔT and WUE under W and HDW was most likely caused by prompt stomata closure (Figure 2E, 2F). A steady increase in ΔT and WUE was observed during three days in D, suggesting that the stress was recognised, and the plant responded by closing stomata followed by immediate recovery when stress was released on day 15 (Figure 2E, 2F). An opposing response was observed in H, where ΔT decreased together with an increase in water consumption, thus indicating enhanced leaf cooling (Figure 2E, Supp. Table 5,6). Overall, it appeared that the drought response became dominant over the heat responses in the physiological responses to HD as indicated by the increase in ΔT and WUE, which both were more similar to drought stress responses as compared to H alone. Also, the physiological analysis uncovered that potato plants were highly susceptible to waterlogging exhibiting a strong reduction in overall plant performance and photosynthetic efficiency and a fast loss of the ability to recover.

Stress combinations and waterlogging have strong effects on potato yield

At the end of the phenotyping, plants were harvested to assess the total biomass accumulation and tuber yield (Figure 2G and 2H). Single H stress led to a slightly higher tuber number (Figure 2G). However, the harvest index was significantly reduced by H as well as by HD, while D alone did not affect final tuber yield (Figure 2H). W strongly inhibited tuber formation and growth and only a few tubers were formed, leading to a significant reduction in the harvest index compared to the control (Figure 2H). A combination of all stress factors abolished tuber formation, reflecting the (near) lethal effect of HDW (Figure 2G, 2H).

Negative effects of the stress treatments on tubers were also observed at the metabolic level (Supp. Figure 2). Thus, starch content was significantly lower under H, HD and W stress, while drought stress alone had no negative impact. The accumulation of hexoses under H and HD may hint at an increased starch degradation and / or to a reduced starch biosynthesis. W caused a strong accumulation of almost all amino acids, most likely caused by protein degradation and a hampered metabolism (Supp. Figure 2).

Molecular responses across omics levels reveal mechanistic insights into multi-stress acclimation

In addition to the morphological and physiological measurements (68 variables, Figure 3D, Supp. Table 1,2), leaf samples were taken for parallel multi-omics analysis. Samples from leaves two and three were pooled, homogenized and used for further analysis (Figure 3A). For each of the treatments the fast response (one day post treatment) and the status at the end of a prolonged stress duration (7 or 14 days of stress) was investigated (sampling points see Figure 1A). While the proteome analysis was untargeted (4258 identified proteins, Supp. Table 3, 4), other omics analyses were targeted comprising 14 pre-selected transcriptional marker genes involved in stress response and tuberisation, 13 phytohormones encompassing abscisic acid (ABA), jasmonic acid (JA), salicylic acid (SA), indole-3-acetic acid (IAA), and their derivatives as well as 22 metabolites comprising amino acids and sugars (Supp. Table 5). To identify processes regulated on proteomics level we performed gene set enrichment analysis (GSEA, Supp. Table 4).

A multi-level data integration protocol was developed to investigate plant signalling and responses across the different omics levels (Figure 3B). After two weeks of waterlogging all plants were dead, therefore only data from the first week could be used in further analyses. The overview of data distribution showed that the most distant physiological state was that of plants exposed to triple stress (HDW): first one week of heat, followed by one week of heat combined with drought, and finally one week of waterlogging (Figure 1 A, 3C, Supp. File 1). Because this triple stress treatment turned out be too harsh and plants were severely affected in both above ground and below ground growth, we also excluded these samples from all further analyses. Next, we reduced the number of variables obtained on phenomics and proteomics levels to equalise numbers of variables across different analysed levels. In order to identify the most informative variables, feature selection using random forest with recursive feature elimination was conducted on the phenomics data, keeping 6 variables for downstream analysis (Figure 3D).

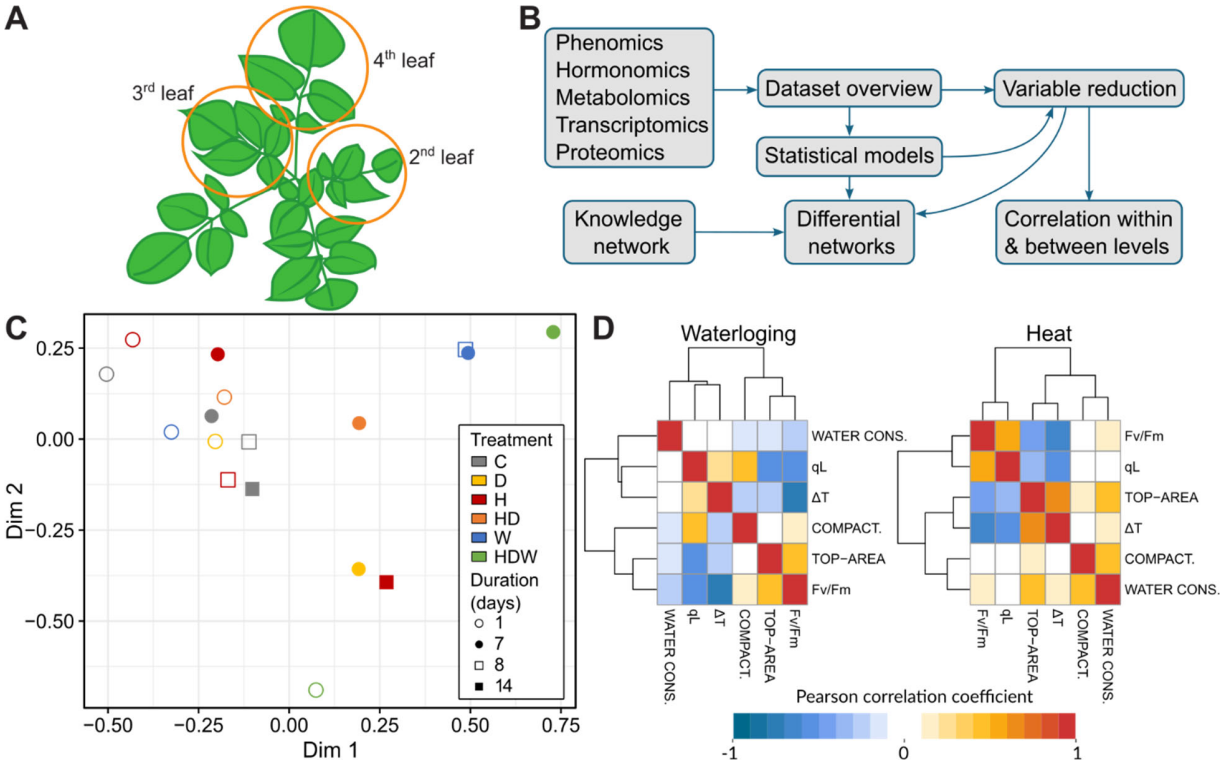

Figure 3: Integrated analysis of measured and generated data permits global visualization and multi-level amalgamation of potato stress responses. A) Schematics of tissue sampling protocol. 2nd and 3rd leaves were harvested for destructive "omics" analysis, 4th leaf was used for relative water content calculation. Remaining plant tissue was quantified to obtain total above-ground biomass and tuber yield. B) Overview of data analysis pipeline. C) Dataset overview: multidimensional scaling shows combined HDW stressed plants as extremes, the centroid of each plant group is shown. D) Most informative variables from the phenomics level. Pearson correlation coefficients between them are presented as hierarchically clustered heat map in waterlogging and heat stress.

The proteomics dataset was reduced to keep only proteins that were identified as differentially abundant in any comparison of stress vs control (135 proteins) and were functionally assigned to pathways that were studied also on other levels (36 proteins, photosynthesis, metabolism of sugars and amino acids, hormone metabolism and signalling, ROS signalling and stress related). Correlation analysis within each level of omics data (see e.g. for hormones and transcripts in Supp. Figure 3A, B) showed that these components are only weakly connected in control conditions, while in both heat or drought, they are highly correlated to each other. More severe stresses, such as the combined heat and drought stress and waterlogging, however, broke this link, suggesting a disorganisation of signalling responses. The canonical correlation analysis between components of different molecular levels similarly showed low connection in control

samples. In stressed samples, blocks of components appeared to be strongly regulated, each specific to a particular stress (Supp. Figure 3C). To capture the events better at the molecular level, variables measured on different levels were integrated into one metabolism and signalling cascades-based knowledge network (Figure 4A). We next superimposed the measured data onto this mechanistic knowledge network and visualised them in parallel for all omics levels per each analysed condition compared to control (Figure 4B, Supp. File 2, Supp. Table 6).

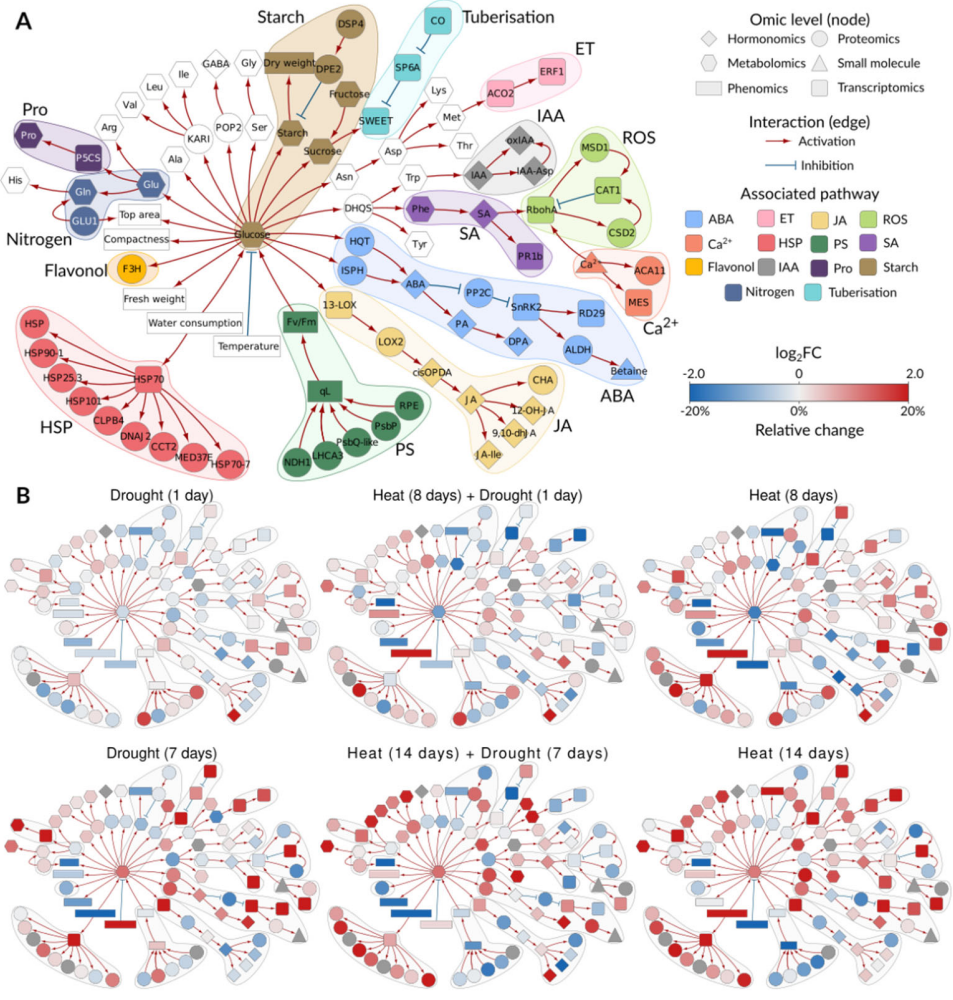

Figure 4: Integration of multi-omics data in a knowledge-based metabolic and signalling network. A) Structure of knowledge network. Individual studied components are coloured according to their function in different pathways. B) To compare the effects of different stresses on the overall state of the plant, we overlaid the knowledge networks with measured changes in component concentration. Nodes are coloured by log2 fold changes (red – increase in stress compared to control, blue – decrease in stress compared to control, grey – measurement not available) shown for two time points: sampling day 8 and sampling day 14 for the different stress treatments, days of stress treatment are given with each network (for more details of the set up see Figure 1A).

This provides an overview of how these stresses rewire biochemical pathways and physiological processes. These were used for interpretation of processes in single and combined H and D stress as well as for waterlogging (W) in next chapters.

Metabolic and molecular responses to individual and combined heat- and drought stress exhibit combinatorial and distinct signatures

While heat stress became effective immediately, drought was applied by water withdrawal on day seven in our set-up and drought stress (30% water capacity of the soil) became effective gradually within three days, visible in the ΔT values (Figure 2E). Similar to previous reports (Demirel et al., 2020; Zaki and Radwan, 2022), we found that Désirée was moderately drought tolerant and exhibited only minor morphological and physiological responses at this moderate stress level and the plants fully recovered when the stress treatment was finished. On the other hand, plants responded to elevated temperatures (heat stress, H) with an upward movement of leaves (hyponasty, Figure 1A), a process known as thermo-morphogenesis (Quint et al., 2016). Previous work showed that heat stress caused an altered biomass allocation between shoots and tubers, with less assimilates allocated to developing tubers (Hancock et al., 2014; Hastilestari et al., 2018), leading to decreased tuber yield and starch accumulation and a decreased harvest index which was also seen in our study (Figure 2H and Supp. Figure 2).

To investigate the effect of stress on leaf metabolism, contents of soluble sugars and starch were measured (Figure 5A). While sucrose levels did not change, there was about twofold increase in the amounts of fructose and glucose after 14 days of H and at day 7 of D and HD. The soluble sugars may act as osmo-protectants under these stress conditions. In addition, we found that protein levels of enzymes involved in sucrose degradation and glycolysis were upregulated in H (at 7 days) and combined HD (day 14) as indicated by gene set enrichment analysis which summarizes the complex proteomics data set (Figure 5B and Supp. Table 4). This may indicate an increased demand for energy and/ or building blocks for stress defence responses. Under these conditions also less starch accumulated, visible at day one and eight in H and at day one HD reflecting lower carbon availability due to a disturbed photosynthesis and/or an increased demand for other processes. Expression of the sugar efflux carrier *SWEET11* was upregulated at the end of both H and D stress presumably to increase sucrose loading into the phloem to counterbalance lower carbon assimilation of source leaves. Considering the reduced

photosynthetic efficiency, these data imply that a lower amount of carbon is assimilated, especially under H and HD, and available for allocation to sink organs, such as growing tubers. This most likely contributes to the impaired tuber growth and lower tuber starch accumulation found under these conditions (Supp. Figure 2).

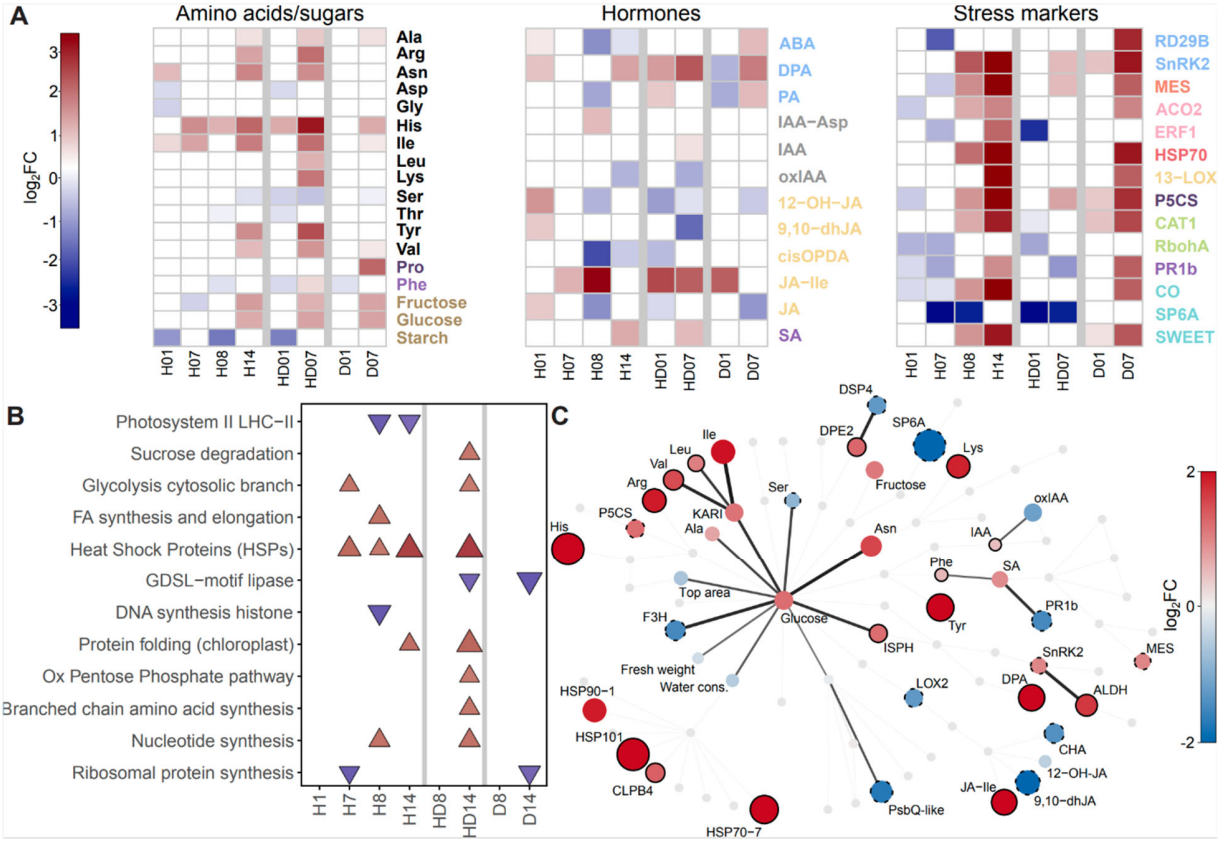

Figure 5: Combined heat and drought stress trigger distinct responses compared to each individual response. Additive effect of combined stress is most pronounced for branched chain amino acids accumulation and JA signalling response. A) Heatmaps showing log2FC (FDR p-value < 0.05) in individual stress heat (H) or drought (D) stress in comparison to combined one (HD) for targeted molecular analyses. Label colours indicate pathway associated with each molecule as in the Knowledge network (see Figure 4 for legend). B) Changes observed on proteomics level. Results of Gene Set Enrichment Analysis (FDR q-value < 0.1) are shown. For more information see Supp. Table 4. D) Biochemical knowledge network showing changes under combined HD stress at day 14 (treatment day 7). In this version of knowledge network, only nodes that were significantly differentially expressed (vs. control conditions) are coloured and the connections between two differentially expressed nodes are coloured black. Node full black border indicates molecules with higher expression levels in HD compared to H and/or D alone. Dashed black border indicates molecules with lower expression levels in HD compared to H and/or D alone (difference of log2FC > 0.5).

One key player stimulating tuberisation and tuber growth is the tuberigen *SP6A*. Its expression was downregulated during the first week of H and in combined HD. During longer heat exposure, expression levels of *SP6A* were similar to control levels, but remained low in HD. Drought alone had little effect on *SP6A*, which is consistent with the low impact on final tuber yield. The transcriptional regulator protein Constans-like 1 (CO) was described to act as a negative regulator of SP6A expression (Abelenda et al., 2016). However, in our experiment, the transcript levels of *CO* did not always change in the opposite direction as *SP6A*, assuming additional regulatory mechanisms. Interestingly, *CO* was upregulated within 7 days of drought stress (D), and it increased with duration of heat, but was unaffected by HD combination (Figure 5A).

Considering the changes in amino acids, the most striking finding was the strongly elevated levels of histidine (His) in all three stress treatments, with the highest amounts detected in combined HD stress. This was accompanied by a significant increase of many (minor) amino acids, in particular iso-leucine (Ile) and other branched chain amino acids (BCAs). This observation was in line with previous reports on combined heat- and drought stress in potato (Demirel et al., 2020). Accordingly, at the proteome level, proteins involved in BCA synthesis were significantly enriched among the ones with increased levels in stress (Figure 5B, C, Supp. Table 3,4).

Proline, which is known as an important regulator of osmotic potential that protects cells by stabilizing proteins and scavenging of reactive oxygen species, was upregulated at day 7 of D stress (sampling day 14) (Figure 5A). This was consistent with the increased transcript levels of *P5CS* (*Pyrroline-5-carboxylate synthase*), the key enzyme for proline synthesis and *RD29* (*Responsive to Desiccation*), both being well-known (drought-) stress marker genes. Consistently, levels of ABA, the key phytohormone that regulates stomal closing and other drought stress responses (Cutler et al., 2010; Zhang et al., 2022), were also elevated after 7 days of D but were clearly reduced in H, while it was not changed in HD stress. Interestingly, the levels of phaseic acid (PA), and dihydrophaseic acid (DPA), two breakdown products of ABA, were lower at one day of D but significantly higher after 7 days in D. The strongest accumulation of DPA levels was detected in the HD treatment, in which DPA levels were elevated already after one day and further increased until the end of the treatment (at day 7). The elevated levels at day one could be explained by the experimental setup, in which the HD treatment started after 7 days of H (that also resulted in DPA accumulation). However, the strong accumulation of ABA breakdown products under D and to even higher level in HD would be in line with their suggested role in long-term acclimation. It was shown that PA, the first degradation product of ABA and the precursor of

DPA, does also activate a subset of ABA receptors (Weng et al., 2016). Because ABA has a very short half-live, it was suggested that the long-lived PA could prime plants for enhanced responses to future drought scenarios (Lozano-Juste and Cutler, 2016).

The phytohormone JA is another typical stress hormone known to be involved in many biotic but also abiotic stress responses (Wasternack and Feussner, 2018). The biologically active form is jasmonyl-L-isoleucine (JA-Ile) and we found strongly increased levels of JA-Ile, basically under all treatments (Figure 5A) except at one and 14 days in H and 7 days in D. 12-Hydroxyjasmonic acid (12-OH-JA) is a by-product of switching off JA signalling with weak signalling activity (Nakamura et al., 2011). It was also described to function as tuber-inducing factor in potato (Yoshihara et al., 1989). Under H, amounts of 12-OH-JA as well as free JA switched from higher amounts measured at day one to lower levels at day 8, and decreased further till the end of the experiment. Also, *cis*-12-oxo-phytodienoic acid (*cis*-OPDA), the biochemical precursor of JA, was detected at much lower levels on day 8 and 14 in H. Both *cis*-OPDA and JA were also reduced at the start of the combined HD (day one) treatment, most likely as a result of prior heat treatment. Altogether, this indicates a strong upregulation in the last step of conjugation for the synthesis of JA-Ile in H, D and HD.

The accumulation of ROS is a detrimental by-product of photosynthesis under heat- and particularly under drought stress conditions. Accordingly, the detoxification of ROS by different enzymes such as catalase or superoxide dismutase together with induction of Ca^{2+} signals is a typical response emerging from stressed chloroplasts (Stael et al., 2015). In line with that, we measured increased transcript levels of catalase (*CAT1*) and a methyl esterase (*MES*), which was selected as Ca^{2+} signalling marker gene (Marc Knight, unpublished data) at the end of the drought and heat treatment (sampling day 14). The transcript levels of *pathogenesis-related protein 1b1* (*PR1b*), a biotic stress as well as drought and salt stress marker (Akbudak et al., 2020) were first lower in H but increased from day 8 to 14 in H and at day 7 in D (Figure 5A). A similar response was seen for the chloroplast-localized lipoxygenase *13-LOX*, which is a well-known marker gene for different stresses, especially chloroplast generated ROS (Bachmann et al., 2002). Strikingly, the response of these genes was less activated or even inhibited when H and D were combined.

Heat stress, but also other stresses, induces the production of heat-shock proteins (HSPs), which is a very conserved process in all organisms. HSPs act as molecular chaperones and play an

important role in maintain the cellular homeostasis and the proteome by supporting protein folding, preventing misfolding or by assisting in the degradation of irreversibly damaged polypeptides (Sato et al., 2024). At transcript level, we observed clearly elevated levels of *HSP70* transcripts after single H and D stress. Under H this was accompanied by an accumulation of numerous HSP proteins as indicated by their significant enrichment among the identified proteins in the proteome approach (Figure 5B, C). This effect was similarly pronounced in combined HD stress (Figure 5C) with a strong enrichment of HSP70, 90, 101 involved in heat stress as well as in assisting folding (Figure 5B). The category “protein folding” comprises mainly HSP70 and 60 group members with many of them that are present in the chloroplast, where they are participate in the repair of photosystem (PS) II components, but also protect proteins such as RuBisCo. In fact, our physiological data indicate a disturbance in the electron-transport chain through PSII under heat. For example, we saw a strong decrease of PSII efficiency under H stress (Figure 2B). The negative effect of H stress is also reflected in lower abundance of photosystem II proteins in the gene enrichment analysis (Figure 5B). More specifically (Supp. Table 3), there were reduced amounts of the PsbQ and PsbP subunits of the oxygen-evolving complex.

Overall, we do see specific stress responses to heat and drought, but also to a combination of both. This becomes also visible in Figure 5C illustrating the signature which is caused by combined heat and drought stress in biochemical pathway view (knowledge network overlaid with multi-omics data). The responses to HD only partly overlap with single D stress, e.g. for the accumulation of DPA. However, for most measured metabolites the patterns are similar to heat, but changes were more pronounced (Figure 5C). Here, we cannot exclude that this domination by heat was linked to rather the mild drought stress level. Interestingly, the transcriptional changes of selected stress-related enzymes were weakest in HD stress combination pointing to a redirection and rearrangement of signalling pathways compared to individual stress factors as suggested by other studies (Zhang and Sonnewald, 2017).

Comprehensive insight into molecular processes mediating the extreme waterlogging sensitivity of potato

Despite being documented as a highly flood-sensitive species, an in-depth characterization of flooding-induced stress responses in potato is sparse (Jovović et al., 2021). The waterlogging sensitivity of potato was evident in the HTP data, with several morpho-physiological traits related to plant performance being negatively impacted following stress imposition (Figure 1C, 2). This included: leaf epinasty, decreased biomass accumulation and shoot elongation, impaired photosynthesis and stomatal conductance as well as a dramatic reduction of tuber yield (see Figure 1,2, Supp. Table 5,6).

Waterlogging significantly affected primary metabolic pathways as reflected in an increase in soluble sugars and free amino acids (i.e. Arg, Leu, Tyr and Val) (Figure 6A). We also observed changes in the expression of stress-associated genes and hormones, thus highlighting potential mechanisms involved in waterlogging acclimation. Waterlogging induced upregulation of the ROS-producing enzyme, *RbohA,* the ethylene biosynthesis gene *ACO2,* and an increase in JA (9,10-dHJA and *13-LOX*) and ABA (ABA, PA, DPA, *RDB29*) metabolism and response. The strong ABA signature observed in waterlogged plants prompted us to compare waterlogging and drought responses (Figure 6A). This revealed common stress-associated responses (e.g.: the induction of *ACO2, RD29B, HSP70)* and a much stronger ABA response in waterlogging relative to drought. Another notable observation was the upregulation of the tuberigen signal, *SP6A* after 1d of waterlogging coinciding with the downregulation of its negative regulator *CO* (Figure 6A).

Proteomics analyses of waterlogged plants revealed mild effects. Six differentially enriched proteins were identified in response to prolonged (7 days, W07) waterlogging treatment. Among the strongly upregulated proteins, were a LAP2-like protein (VdnPW4_5460) which encodes an aminopeptidase, two glucan endo-1,3-beta-glucosidases (VdnPW4_8729, PBdnRY1_427), a POP2-like protein encoding a GABA transaminase and a SEC31B-like protein, previously described as a component of coat protein complex II (COPII), involved in RT-derived transport vesicles (Li et al., 2021). Waterlogging led to the downregulation of the chloroplast ribosomal protein RPL27-like, demonstrated to be important for protein synthesis (Figure 6B).

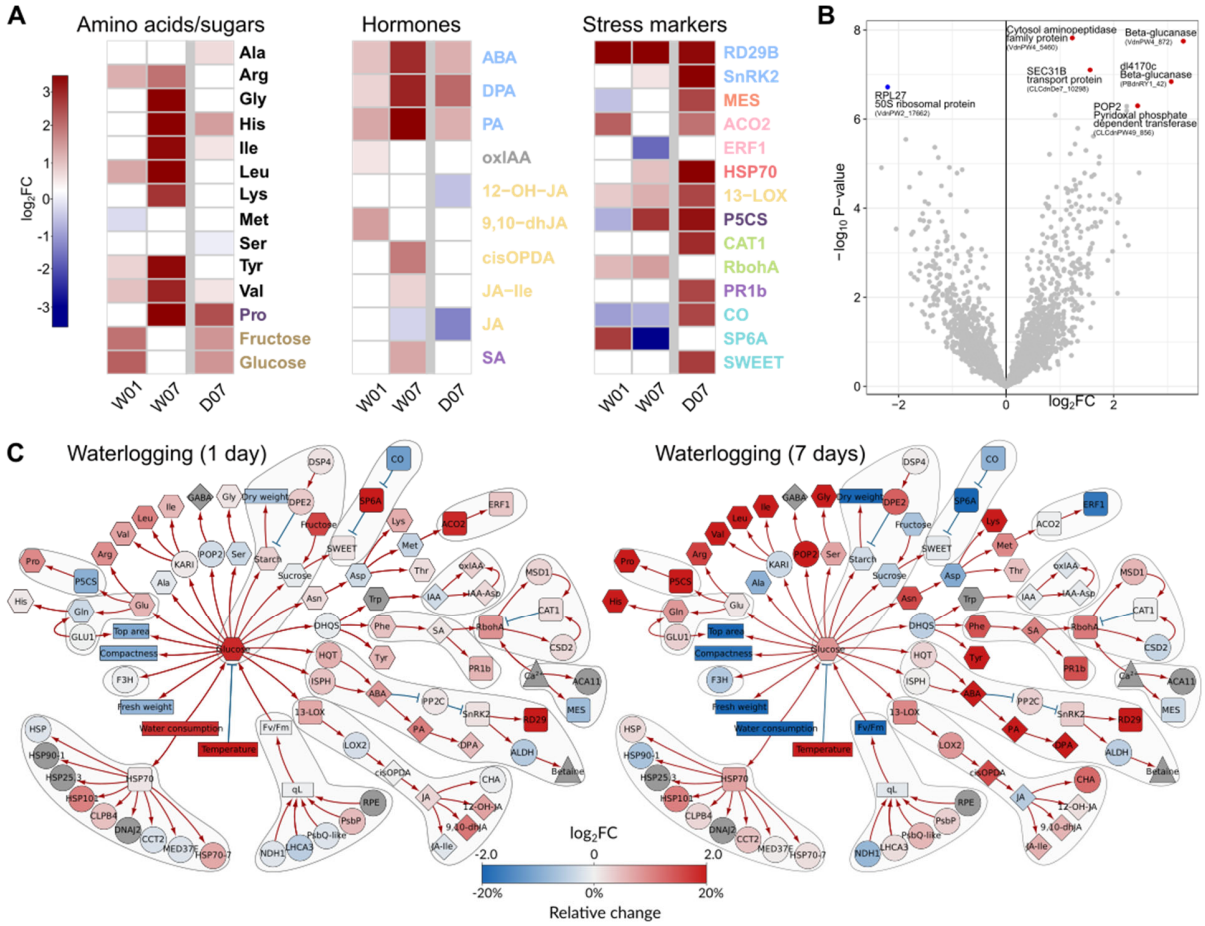

Figure 6: Waterlogging triggers drought-stress like molecular responses in potato. A) Heatmaps showing log2FC (FDR p-value < 0.05) B) Volcano plot of differential proteomics analysis at day 7. Proteins with FDR p-value < 0.05 shown as blue (downregulated) and red (upregulated) dots. For more information see Supp. Table 3. C) Knowledge network of waterlogging stress at day 1 and day 7 (unfiltered, colour range [-2, 2]). For legend see Figure 4.

The multi-level integrative analyses enabled visualization of the progression of stress symptoms in waterlogged plants. In comparison to one day of waterlogging, molecular responses to prolonged waterlogging stress (7 days, W07) displayed a distinct signature (Figure 6C). While ABA-, JA- and ROS-biosynthesis and accumulation of free amino acids was further increased, we observed that prolonged waterlogging led to increased SA levels and a general inhibition of the tuberisation process (i.e. *SP6A* downregulation). In addition, genes related to ethylene biosynthesis and response were not regulated (*ACO2)* or downregulated (*ERF1),* thus suggesting temporal control of ethylene signalling. Despite representing opposite ends of the water stress

spectrum, waterlogging and drought, elicited significantly overlapping responses, notably related to ABA metabolism and proline accumulation (Figure 6A, C).

Altogether, the multi-level integrative analysis revealed key early and late biochemical, physiological and molecular responses to waterlogging stress in potato. It allowed the identification of temporal differences, thus providing insight into potential factors causing the observed susceptibility of potato to waterlogging. It revealed overlapping molecular responses to water extremes (waterlogging vs. drought) which can be significant for future studies on fluctuating water stresses in this crop.

DISCUSSION

There has been significant progress in the last decades in our understanding of how plants perceive and respond to abiotic stresses, especially in the context of crop-appropriate cultivation techniques and precision agriculture. The advent of next-generation sequencing has resulted in the availability of an increasing number of high-quality crop genomes including potato (Leisner et al., 2018; Petek et al., 2020; Pham et al., 2020; Hoopes et al., 2022). This, coupled with high-throughput technologies and advanced gene editing tools, offer unprecedented possibilities to gain insight into the complex signalling pathways and molecular components regulating various stress tolerance traits.

Despite its outstanding importance as a major food crop, research into the vulnerability of potato to abiotic stresses lags behind that of other staple crops. In recent years, potato yields have been significantly affected by heat, drought, and flooding, often occurring sequentially or simultaneously (Dahal et al., 2019; Jovović et al., 2021; von Gehren et al., 2023). Considering the increasing occurrence of these extreme weather events, this knowledge gap needs to be urgently addressed. In this study, we leveraged the power of several omics' techniques and their integrated analysis to build a comprehensive global picture of potato responses to single and combined heat, drought, and waterlogging stress.

Leveraging multi-omics data integration to capture the complexity of biological systems

Several tools are already available to integrate omics data collected on multiple molecular levels (Joshi et al., 2024). Most broadly used are the mixOmics package (Rohart et al., 2017; Singh et al., 2019), integrating datasets based on correlations and/or pathway visualisation tools such as

PaintOmics (Liu et al., 2022). In this study, we integrated five omics-level datasets. Such complex datasets are rarely available even in medical research (Lee et al., 2019), and in most studies only two to three omics datasets were combined (Ployet et al., 2019; Lozano-Elena et al., 2022; Núñez-Lillo et al., 2023; Núñez-Lillo et al., 2024; Sinha et al., 2024). Since the existing tools were not directly suitable for analysis of datasets with that many levels of omics data, here we developed a novel pipeline harnessing the potential of both (integrative and visualization) approaches. An additional step was introduced to reduce the number of variables. This reduction of variables was especially important for the correlation analyses across omics levels, where we kept only the most informative variables. In the first step, we performed statistical modelling and correlation analyses, which provided partial overview of events. In the second step, mechanistic insights were obtained by generating a customised biochemical knowledge network. Our network was constructed based on the knowledge extracted from different databases, most notable Stress Knowledge Map (Bleker et al., 2024) and KEGG (Kanehisa et al., 2017) and from literature to integrate all components that were kept after variable selection. The obtained biochemical knowledge network enabled a comprehensive overview of events in the pathway setting and thus the identification of mechanistic differences occurring in the response to different stresses. Our novel pipeline is thus setting the basis for the integration and the interpretation of complex datasets in future studies and can be also applied to other species.

Integrative omics provides global insights into potato abiotic stress responses

While multi-omics approaches have been successfully applied in numerous crop species, our study is the first to do so in potato. We subjected the cultivar Désirée to waterlogging, drought, heat, a combination of heat and drought, and triple stress combination encompassing all three. Across each stress treatment, detailed morpho-physiological traits were measured, with a subset of plants sampled for the probing of a diverse array of molecular stress markers, hormones, metabolites, and proteome analyses across several time points.

In general, stress combinations appeared to be more detrimental to the plant performance than individual stress applications. The combination of H, D and W led to a rapid decline in plant viability and eventually most plants died. However, all individual stress factors caused a reduced plant growth, had a negative impact on photosynthetic assimilate production, and both heat and waterlogging stress impaired tuber yield (Figure 7) and tuber starch accumulation (Suppl. Figure 2). Considering all stress responses, it turned out that the cultivar Désirée was less affected by

the applied drought stress indicating that it is quite resilient to drought as suggested previously (Demirel et al., 2020). A combination of heat and drought caused stronger growth retardation than both stresses alone with drought responses overwriting heat adaptations at physiological level.

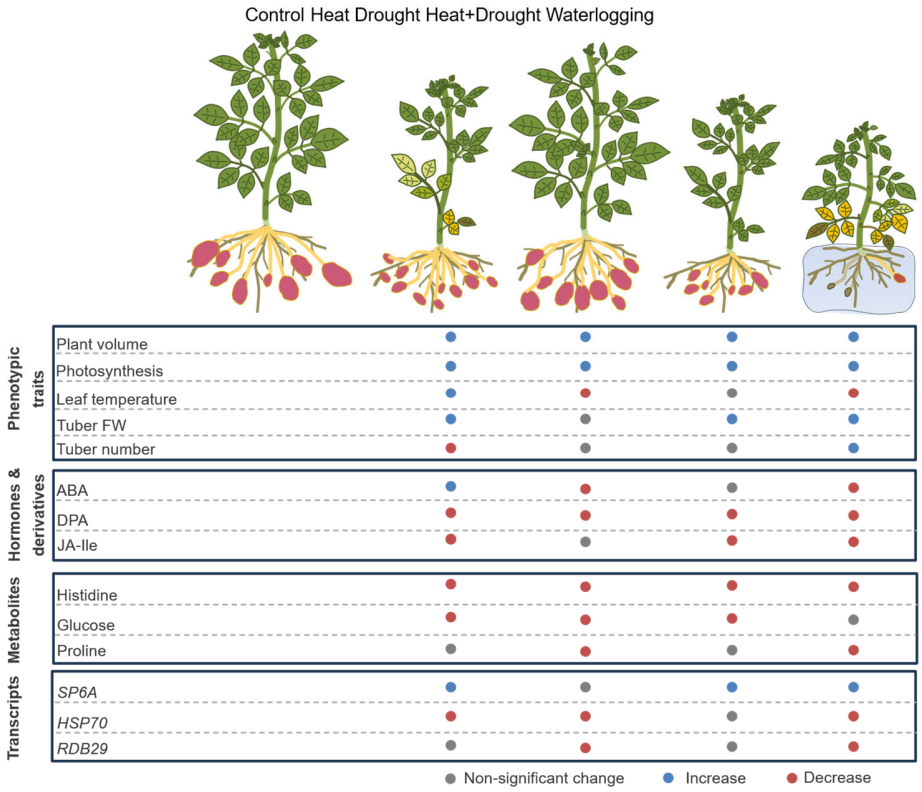

Figure 7. Schematic summary of multilevel responses to single and combined heat, drought and waterlogging stresses. Selected variables from each level are shown. Summary of molecular responses (hormones, metabolites and transcripts) was based on the comparisons illustrated in Figures 5 and 6. Summary of morphophysiological responses were based on the data from the last day of the experiment (Day 28), which includes tuber information. Proteomics data set is not included here due to the small dataset of differentially expressed proteins in the waterlogging treatment. Degree of increase or decrease is not specified.

Nevertheless, despite the apparent mild drought phenotypes, a clear drought-associated signature (accumulation of sugars, proline, histidine and most stress-induced transcripts) confirmed the activation of stress responsive pathways, particularly at day 7, which apparently contributed to stress acclimation (see Figure 7). Thus, we detected the activation of the ABA response pathway, in terms of an increase in the hormone and its degradation products, as well as in related metabolites, like proline, and the selected ABA-responsive marker genes *SnRK*, *P5CS*, *RD29B*, leading to the corresponding physiological responses (e.g. decreased water-use

and leaf temperature caused by stomata closure). Particularly interesting was the accumulation of the ABA catabolite DPA at later time points. The precursor of DPA, PA was suggested to have an important role in priming for increased resilience to future drought stress in Arabidopsis (Lozano-Juste and Cutler, 2016). It is believed that DPA does not trigger ABA responses, but that has to our knowledge not been studied in potato. Hence, it might be that DPA acts as priming signal for stress acclimation and resilience in potato.

Compared to drought, heat stress caused stronger effects on Désirée plants at all levels from growth to photosynthesis and yield. Thermomorphogenesis is a well-described growth response to elevated temperature stress comprising shoot elongation and hyponastic movement of leaves which together with an increased transpiration are seen as an acclimation to increase ventilation and to cool the aboveground part (Quint et al. 2016). In our study, we clearly observed the hyponastic movement of leaves, stomatal opening and a decrease in ΔT (Figure 7). This physiological response was accompanied by a decreased amount of ABA. In contrast, the heat-mediated shoot elongation that has been seen in other potato varieties was not visible (Hastilestari et al., 2018; Tang et al., 2018). Instead, the plant height of cv. Désirée plant was even reduced under elevated temperature suggesting cultivar-specific differences that can be exploited in further studies to entangle different morphological stress adaption mechanisms in potato. In *A. thaliana*, the thermomorphogenic hypocotyl elongation is tightly linked with an increase in auxin levels and is mediated by the transcription factor Phytochrome interacting factor 4 (PIF4) (Quint et al. 2016). Consistent with the morphological response, we did not find significantly altered levels of the phytohormone IAA in leaves of Désirée plants in response to heat (Figure 5). High temperature treatment negatively affects photosynthetic capacity, in particular, the efficiency of photosystem II, which is in line with the results of other studies (see (Mathur et al., 2014) for review) and was seen here at both physiological and proteomic levels. In a previous study by (Hancock et al., 2014), which also used cv. Désirée, the net CO_2 assimilation was even higher under elevated temperatures than in control conditions. This difference might be related to the different set-up, as in the latter study the night temperature was kept at 20°C, while here it was adjusted to 28°C, suggesting that it plays an important role in maintaining photosynthetic activity.

The heat-induced impact on photosynthetic capacity was also reflected by a lower production of assimilates, indicated by the decreased amount of transitory starch. Concomitantly, contents of hexoses were found to be increased consistent with earlier studies (Hastilestari et al. 2018). This

increase may contribute to the osmo-protection of cells and provides energy for the costly heat stress response such as the formation of heat shock proteins (Guihur et al., 2022). In fact, a massive accumulation of heat-shock proteins was found after one week of heat stress, together with elevated levels of *HSP70* transcript levels at day 8 and much stronger at day 14 (Figure 5). Although energy-demanding, the induction of HSP is important for the cellular homeostasis and to maintain growth and metabolism at elevated temperatures. This is well demonstrated by transgenic potato plants with increased expression of a beneficial allele of *HSC70*, that led to improved heat stress tolerance (Trapero-Mozos et al., 2018).

A downregulation of photosynthesis is a typical stress response to prevent potential damage, for example caused by ROS. This has strong implications on plant growth and yield and is therefore regulated at various levels including light-harvesting and electron transport with high implications for crop improvement (Kromdijk et al., 2016), particularly under stress conditions (Grieco et al., 2020). The resulting lower photosynthetic capacity together with an increased energy demand for stress defence reduces the amounts of assimilate that can be translocated toward the developing tubers and its availability for storing starch. Beside assimilates, molecular signals stimulate tuber development and growth. One important regulator is *SP6A* which was down-regulated at transcript level in our studies, similar to previous ones (Hancock et al., 2014; Lehretz et al., 2020; Park et al., 2022; Koch et al., 2024). Stem-specific overexpression can overcome heat-mediated yield reduction and enhances delivery of assimilates towards tuber. Nonetheless, it is not sufficient to achieve heat-stress resilient plants, as *SP6A* overexpressing plants exhibited above-ground growth penalties (Koch et al., 2024). Hence more research and additional (global) approaches are required to increase our understanding.

Looking at plant hormones, we observed changes of stress hormones like SA and JA, that traditionally have been associated with biotic stress responses. Quite striking in this context was the increase in amount of JA-Ile under heat, drought and the combination of both (Figure 5). This is consistent with previous observations reporting that JA has a positive effect on thermotolerance (Clarke et al., 2009; Balfagon et al., 2019). In Arabidopsis JA-Ile accumulation was also observed under drought (Yoshida and Fernie, 2024). Heat stress increased levels of OPDA, JA and JA-Ile and application of 5µM methyl-jasmonate improved cell viability (Clarke et al., 2009). Using mutants this study also showed, that JA acts in concert with SA in conferring thermotolerance. Recently, it was also shown that increased levels of JA-Ile resulted in improved drought stress tolerance in Arabidopsis (Mahmud et al., 2022). Therefore, JA metabolism seems as promising

target for future engineering of abiotic stress tolerance in potato but a deeper understanding of regulatory factors is required, particularly in the context of cross-talk and links to organellar functions such as photosynthesis (Bittner et al., 2022).

Extreme sensitivity to waterlogging in potato – integrative -omics highlights commonalities with drought

Our study provides the first detailed insight into the molecular responses underlying the high vulnerability of potato to waterlogging. Water saturation imposes rapid oxygen deficiency in the soil, thus impairing root respiration and function. Plant survival in flooded soils involves various morphological and metabolic responses to either escape or cope with hypoxia, which involve acclimation responses in roots but also in aerial organs (Sauter, 2013; Leeggangers et al., 2023).

The data showed that plant growth and performance were more drastically affected by waterlogging as compared to H, D and HD treatments. In addition, HTP data suggests that waterlogging had a dominant effect even when applied after a previous combined exposure to heat and drought (HDW) (Figure 1C and 2). When applied as a single stress, detrimental effects on plant performance increased over time. Waterlogging dramatically impairs root conductance and water and nutrient uptake, causing tissue dehydration and wilting. This triggers water-saving responses such as stomatal closure and epinasty, which were reflected in increased leaf temperatures and reduced plant compactness, respectively (Supp. Figure 5). Epinastic leaf movement, a common waterlogging response in *Solanaceae*, is thought to reduce photosystem damage by irradiation and transpiration (JACKSON and CAMPBELL, 1976; Geldhof et al., 2023). Both stomatal conductance and epinasty are regulated by the pivotal flooding signal ethylene (Leeggangers et al., 2023). While ethylene levels were not measured here, the analyses of synthesis genes (i.e.: *ACO2)* suggested the activation of ethylene production in waterlogged shoots. Ethylene is also known to trigger *RBOH* expression and can act synergistically with ABA to reduce stomatal conductance (Zhao et al., 2021). ABA is also considered to signal root stress during waterlogging (JACKSON and HALL, 1987; Zhao et al., 2021). We observed both the activation of ABA signalling and ABA accumulation and together with increased levels of proline, this is consistent with a strong drought signature (Figure 6A, 6C). Paradoxical, waterlogging is known to elicit shoot drought responses. As root function in hypoxic soil ceases, it triggers a ‘drought like’ response in the shoot with the goal to trigger water saving measures. A focus on this

ABA and drought-mediated regulatory network might thus be an attractive target for probing common resilience mechanisms to both precipitation extremes.

The energy shortage caused by waterlogging also leads to significant changes in sugar metabolism. The accumulation of soluble sugars such as glucose and fructose, might be a consequence of sink-source imbalances during waterlogging and thereby, a decline in shoot-to-root sugar transport. Strikingly, we observed upregulation of *SP6A,* a positive regulator of tuberisation, thus suggesting potential roles of this gene in short-term responses to waterlogging.

Prolonged exposure to waterlogging revealed several aspects of late responses and factors contributing to potato susceptibility to waterlogging. Leaves of waterlogged plants overcome energy shortages by recycling carbon from amino acids and GABA (Wu et al., 2021, Lothier, 2020 #94). The latter, plays an important role not only in TCA replenishment but also in ion homeostasis and reduction of oxidative stress (Wu et al., 2021). We observed a strong increase in free amino acids that, together with the upregulation of POP2 and an aminopeptidase (Figure 6), suggests increased protein breakdown and utilization of amino acids as alternative energy sources. Furthermore, the downregulation of RPL27 (and other ribosomal proteins) could indicate the shutting down of energy-demanding processes, such as protein synthesis, as a response to this energy shortage.

Potato susceptibility to prolonged waterlogging was evidenced by other multi-level events such as the upregulation of proteins related to protein and cell wall component turnover, SA levels, *RboHA* upregulation and photosynthesis impairment (Figure 2, Supp. Figure 3, Figure 6). It is also explained by increased ABA signalling and biosynthesis and *RBohA* expression, which convergently indicate increased tissue dehydration and oxidative stress that is reflected in the HTP data (Figure1C, Figure 2). This includes decreased tuber number and weight, indicating a retardation of both tuber initiation and bulking. As tuberisation is a particularly energetically expensive process, the imposition of root zone hypoxia likely disrupts the underground sink strenghth essential for stolon development, tuber initiation and bulking.

Altogether, our data suggest that two weeks of waterlogging led to near-lethal effects, and even if acclimation responses were activated, overall, they could not compensate for maintaining root function (i.e. unrecovered water consumption, Supp. Table 5) and plant survival, even during recovery, thus confirming the high susceptibility of potato to waterlogging.

Conclusion

The present comprehensive approach produced a rich integrated dataset, which enabled exploration of molecular mechanisms across various levels and processes. Through the connection of phenotype to molecular responses, we attained deeper insights into the intricate regulation of metabolic and phenotypic traits. This should now guide the identification of key regulators that govern the interplay between molecular dynamics and their phenotypic expressions. The utilization of both knowledge-based approaches and multivariate statistical methods played a crucial role in deciphering complex molecular regulatory networks and their association with phenotypic and physiological traits, thereby facilitating the rapid generation of hypotheses.

In addition to several novel insights into potato stress responses, this study also provides a blueprint for performing and analysing single and multiple stress and effective integration of large datasets for potato. Importantly, this setup could be applied also for other plant species. These advancements hold significant implications for potato breeding strategies, providing a deeper understanding of plant stress responses and expediting trait selection. As agricultural landscapes confront challenges like climate change and population growth, embracing multi-omics integration holds promise for cultivating resilient potato varieties that can thrive in various conditions.

METHODS

Plant growth conditions and sampling

150 in-vitro potato cuttings (*Solanum tuberosum* cv Désirée) were cultivated in fully saturated 250 ml pots filled with 95 g of commercial peat substrate (Klassman 2, Germany) under controlled conditions. 2-weeks old seedlings were transplanted into 3L PSI pots (15.5 cm diameter, 20.5 cm height) filled with 1600 g of the same substrate, mixed with sand in a 3:1 proportion. The soil surface was covered with blue rubber mat. The climate conditions in the Walk-in FytoScope growth chamber (FS-WI, Photon Systems Instruments (PSI), Drásov, Czech Republic) during cultivation were set at 22/19 °C for day/night temperature with 60% relative humidity (RH) and growing light intensity at 330 µmol m^{-2} s^{-1} photosynthetic photon flux density (PPFD) (55% cool-white LED and 85% far-red LED lighting as determined with SpectraPen MINI (PSI, Drásov, Czech Republic)). The plants were grown under long-day conditions (16 h photoperiod) and were regularly watered to maintain soil relative water content at 60% field capacity (FC).

After 32 days of cultivation, plants were randomly distributed into 6 groups (6 plants each) referring to control group and 5 different stress conditions (heat, drought, combined heat and drought, waterlogging and combination of heat, drought and waterlogging) (Figure 1). Plants were moved into two growth units of Growth Capsule (GC, PSI, Drásov, Czech Republic) where climate conditions for day/night temperature were set in one unit to 22/19°C, referring to control conditions, and in the second unit to 30/28 °C, referring to heat conditions. In both units growing light intensity was set at 330 µmol m^{-2} s^{-1} PPFD (72 and 19% cool-white LED and 10 and 13% far-red LED control) and relative humidity was maintained at 55%. Three water regimes were applied: 60% FC in control conditions, 30% FC in drought conditions and 130% FC in waterlogging conditions. All plants were measured under control in day 0 then the stress treatments depicted schematically in Figure 1. The treatments were applied as the following: (1) Control conditions – cultivation at 22/19 °C, watering up to 60% FC; (2) Drought conditions – cultivation at 22/19 °C, watering up to 60% FC until day 7, then reduce watering to 30% FC for 1 week (until day 14); (3) Heat conditions – cultivation at 30/28 °C for 2 weeks, watering up to 60% FC until day 14; (4) Heat + Drought conditions - cultivation at 30/28 °C for 2 weeks, watering up to 60% FC for 1 week (until day 7), then reduce watering to 30% FC for 1 week (until day 14); (5) Waterlogging conditions – cultivation at 22/19 °C, watering up to 130% FC for 2 weeks (until day 14); (6) Heat + Drought + Waterlogging conditions – cultivation at 30/28 °C for 2 weeks with watering up to 60% FC for 1 week (until day 7), then reduce watering to 30% FC until day 14 followed by inducing waterlogging by cultivation at 22/19 °C for 1 week with watering up to 130% FC until day 21. Except for Heat + Drought + Waterlogging conditions, all stress treatments were followed by one week of recovery (from day 15 and until day 21) in control conditions.

Plants were divided into two sets, “phenotyping plants” and “plants for tissue harvest” (see Suppl. Table 1). Phenotyping set consisted of 6 replicates per treatment, in total 36 plants, and was used for daily image-based phenotyping (for definition of scored traits see Suppl. Table 2). Harvest set, in total 112 plants with 4 replicates per sampling time point and treatment, was used for successive harvesting of 2nd and 3rd youngest fully developed leaves for follow-up transcriptomics, metabolomics, hormonomics, and proteomics analyses. The 4th leaf was harvested to measure the relative water content (Supp. Table 5).

High-throughput phenotyping

Prior to the stress treatment initiation and during the stress treatments, all plants were daily phenotyped using a complex phenotypical protocol consisting of the acquisition of (1)

photosynthesis-related traits by using kinetic chlorophyll fluorescence imaging; (2) measurement of temperature profiles of the plants by thermal imaging; (3) morphological, growth and colour-related traits (Suppl. Table 2) by using top and multiple angles side view RGB imaging; with all sensors for digital analysis being implemented in the PlantScreen™ Modular system (PSI, Drásov, Czech Republic). Each pot was loaded onto a transport disk automatically moving on a conveyor belt between the automatic laser height measuring unit, acclimation unit, robotic-assisted imaging units, weighing and watering unit, and the cultivation greenhouse located area. The raw data were automatically processed through the PlantScreen™ Analyzer software (PSI, Drásov, Czech Republic).

Visible RGB imaging

To assess morphological traits, RGB imaging was used based on side-view imaging from three angles (0°, 120° and 240°) (RGB1) and top-view imaging (RGB2). In the RGB imaging unit, two RGB cameras (top and side) were mounted on robotic arms with a rotating table with precise angle positioning, and LED-based lighting source supplemented with each camera to ensure homogeneous illumination of the imaged plant. RGB images (resolution 4112 × 3006 pixels) of the plants were captured using the GigE PSI RGB – 12.36 Megapixels Camera with 1.1” CMOS Sensor (PSI, Czech Republic) from the side and top view. For the side view projections, line scan mode was used with a resolution of 4112 px/line, 200 lines per second. The imaged area from the side view was 1205 × 1005 mm (height × width), while the imaged area from the top view position was 800 × 800 mm. The digital biomass of each plant was automatically extracted with the PlantScreen™ Analyzer software (PSI, Drásov, Czech Republic) and processed as described by (Awlia et al., 2016). The plant volume (Klukas et al., 2014) and relative growth rate (Paul et al., 2019) were calculated (Suppl. Table 2).

Chlorophyll fluorescence imaging

An enhanced version of the FluorCam FC-800MF pulse amplitude modulated (PAM) chlorophyll fluorometer (PSI, Drásov, Czech Republic) was used for the non-invasive assessment of photosynthesis. In the chlorophyll fluorescence imaging unit, a TOMI-2 high-resolution camera (resolution of 1360 × 1024 px, frame rate 20 fps and 16-bit depth) with a 7-position filter wheel is mounted on a robotic arm positioned in the middle of the multi-colour LED light panel with dimensions of 1326 x 1586 mm. The LED panel was equipped with 4 × 240 red-orange (618 nm), 120 cool-white LEDs (6500 K) and 240 far-red LEDs (735 nm) distributed equally over an imaging

area of 80 × 80 cm. Prior to chlorophyll fluorescence imaging, plants were transported through the acclimation tunnel equipped with cool-white LEDs (6500 K), where they were adapted 5 min to the light as described in (Findurová et al., 2023). The light intensity (Photosynthetically Active Radiation, PAR) of the LED light source (cool-white actinic light, PSI, Drásov, Czech Republic) used for the adaptation and chlorophyll fluorescence measurement was 500 µmol m^{-2} s^{-1}. The measuring protocol was set as the following: 3 s of cool-white actinic light at 500 µmol m^{-2} s^{-1} was applied to determine the steady-state F-level in the light-adapted state (F_t_Lss) followed by an 800 ms saturation pulse of 3200 µmol m^{-2} s^{-1} to determine the maximum fluorescence in the light-adapted state (F_m_Lss). Afterward, the actinic light was turned off, far-red light (735 nm) was turned on and photosystem II (PSII) were relaxed in the dark for 800 ms to determine the minimum fluorescence in the light-adapted state (F_0_Lss). Parameters extracted using the PlantScreen™ Analyzer software (PSI, Drásov, Czech Republic) were the operating efficiency of photosystem II (QY_Lss known as Φ_{PSII}) determined as (F_m_Lss- F_t_Lss)/F_m_Lss, Lss referring to light steady state, fraction of open reaction centers in PSII (oxidised QA) (qL_Lss) determined as (F_q_Lss/F_V_Lss) * (F_0_Lss/F_t_Lss) and maximum efficiency of PSII photochemistry of light-adapted sample in steady-state (F_v/F_m_Lss) determined as F_v_Lss/F_m_Lss (Supp. Table 2).

Thermal imaging

Thermal IR images were obtained using InfraTec thermal camera (VarioCam HEAD 820(800)) with a resolution of 1024 × 768 pixels, thermal sensitivity of < 20 mK and thermal emissivity value set default to 0.95. The IR imaging box contained camera mounted on a side view oriented robotic arm for side view imaging, a rotating table with precise plant positioning and an automatically controlled heated wall on the opposite side to the thermal camera. PT1000 temperature sensors integrated inside of the wall were used for automatic feedback controlled heated wall temperature with an offset of 8°C above the ambient temperature to increase the contrast during the image processing. The thermal images were acquired in darkness using line scan mode as described in (Findurová et al., 2023) with a scanning speed of 30 Hz and each line consisting of 768 pixels. The imaged area was 1205 × 1005 mm (height × width). PlantScreen™ Analyzer software (PSI, Drásov, Czech Republic) was used for the automatic extraction of leaf surface temperature as described (Abdelhakim et al., 2021). In order to avoid the influence of ambient conditions, the obtained leaf surface temperature was normalised by subtracting the ambient air temperature, yielding the temperature difference (ΔT).

Tissue sampling

Harvest set of plants, in total 112 plants with 4 replicates per sampling time and treatment, was used for successive harvesting of 2nd and 3rd youngest fully developed leaves on day 1, 7, 8, 14, 15, and 21 after stress treatment initiation (Treatment days). Single leaf tissue was flash-frozen in liquid nitrogen. Subsequently, tissue was homogenised, aliquoted and distributed for individual -omics analysis. Remaining above-ground tissue was harvested and total fresh weight (FW) and dry weight (DW) were defined. On the last day of the experiment, the 4th leaf was harvested, and three leaf disks were collected and weighed, then soaked in water to determine the turgor weight (TW) and dried in the oven to calculate the relative water content (RWC) calculated as the following: RWC = (FW − DW)/(TW − DW). In addition, the below ground tissue was collected, where number of tubers per plant and total weight were assessed from four replicates per treatment. Harvest index was calculated as a ratio between tuber weight and the total biomass.

Multi-omics analysis

Transcriptomic marker analysis

RT-qPCR was performed to assess the expression of 14 marker genes involved in redox homeostasis (RBOHA, CAT1), hormonal signalling - ethylene (ACO2, ERF1), abscisic acid (P5CS, SnRK2.9, RD29B), cytokinin and salicylic acid (PR1b), jasmonic acid (13-LOX), heat stress (HSP70), tuber development (SWEET, SP6A), circadian clock (CO) and calcium signalling (MES, methyl esterase, Marc Knight, unpublished data), using EF1 and COX as previously validated reference genes (Supp. Table 7).

RNA was extracted and DNase treated using Direct-zol RNA Miniprep Kit (Zymo Research, USA) from 80-100 mg of frozen homogenised leaf tissue, followed by reverse transcription using High-Capacity cDNA Reverse Transcription Kit (Thermo Fisher, USA). The expression of the target and reference genes was analysed by qPCR, as described previously (Petek et al., 2014; Abdelhakim et al., 2021). QuantGenius (http://quantgenius.nib.si), was used for quality control, standard curve-based relative gene expression quantification and imputation of values below level of detection or quantification (LOD, LOQ) (Baebler et al., 2017).

Hormonomics

Concentration of the endogenous abscisate metabolites (ABA, PA, DPA, neophaseic acid, neoPA), auxin metabolites (free IAA, its conjugate IAA-Aspartate, IAA-Asp and catabolite 2-oxindole-3-acetic acid, oxIAA), jasmonates (JA, JA-Ile, 9,10-dhJA, 12-OH-JA, *cis*-OPDA) and salicylic acid (SA) were determined in 10 mg of plant material according to the method described (Flokova et al., 2014) and modified by Široká et al. (Siroka et al., 2022). All experiments were repeated as four biological replicates. The samples were extracted in cold 1 mL of 1 mol/L formic acid in 10% aqueous methanol with the addition of internal stable isotope-labelled standards (5 pmol of [$^{13}C_6$]-IAA, [$^{13}C_6$]-oxIAA, [$^{13}C_6$]-IAA-Asp, [$^{13}C_6$]-IAA-Glu and [$^{2}H_2$]-(-)-JA-Ile, 10 pmol of [$^{2}H_5$]-OPDA, [$^{2}H_6$]-JA and [$^{2}H_6$]-ABA, and 20 pmol of [$^{2}H_4$]-SA) and whole extracts were purified on Oasis HLB solid phase extraction columns (1cc/30 mg, Waters) following the described protocol (Flokova et al., 2014). The analysis was performed on a 1260Infinity II LC/SFC hybrid system, coupled to an Agilent 6495B Triple Quadrupole LC/MS system (Agilent Technologies, Santa Clara, CA, USA) using the settings described (Siroka et al., 2022).

Metabolomics

For determination of soluble sugar, starch and amino acid contents, 30 - 50 mg of freeze-dried leaf or tuber material were extracted with 1 ml of 80% (v/v) ethanol and incubated at 80°C for 60 min. After centrifugation for 5 min at 13,000 rpm, cleared supernatants were transferred into new tubes and evaporated to dryness at 40°C. The residue was resolved in 300 µl of water and used for the determination of soluble sugars and amino acids. The pellet was used to determine the starch content. The pellet was subsequently incubated with 0.2 M KOH at 95°C for 1 h. The pH value was adjusted to 5.5 by adding 1 M acetic acid and the starch was digested to glucose by treatment with amylogucosidase (1 mg/ ml in 50 mM sodium acetate buffer) overnight. The amount of soluble sugars was determined photometrically as described previously (Smith and Zeeman, 2006). For the determination of amino acid contents, 10µl of extracts were mixed with 80 µl borate buffer (200 mM, pH 8.8) and derivatized with 10µl aminoquinolyl-N-hydroxysuccinimidyl carbamate (AQC) solution by heating it 55°C for 10 min. Subsequently the samples were measured and quantified using standard samples on a Dionex P680-HPLC system with an RF 2000 fluorescence detector (Dionex, Sunnyvale, CA, USA) as described elsewhere (Obata et al., 2020).

Proteomics

For high-throughput analysis a shotgun proteomics method (Hoehenwarter et al., 2008) was performed with modifications. 40 mg of leaf tissue from multiple stress conditions were freeze-dried in liquid N_2 and ground using mortar and pestle. The proteins were extracted, pre-fractionated (40µg of total protein were loaded onto the gel (1D SDS-PAGE), trypsin digested and desalted (using a C18 spec plate) according to a previously described method (Chaturvedi et al., 2013; Ghatak et al., 2016). Prior to mass spectrometric measurement, the tryptic peptide pellets were dissolved in 4% (v/v) acetonitrile, 0.1% (v/v) formic acid. One µg of each sample (3 biological replicates for each cell type) was loaded onto a C18 reverse-phase analytical column (Thermo scientific, EASY-Spray 50 cm, 2 µm particle size). Separation was achieved with a two-and-a-half-hour gradient method and was set to 4 - 35% buffer B (v/v) [79.9% ACN, 0.1% formic acid (FA), 20% Ultra high purity (MilliQ)] for 90 minutes and then to 90% buffer B over one minute, and remained constant for an additional 8 minutes. The buffer A (v/v) was 0.1% FA in high purity water (MilliQ). The flow rate was set to 300 nL min−1. LC eluent was then introduced into the mass spectrometer (Q-Exactive Plus, Thermo Scientific) through an Easy-Spray ion source (Thermo Scientific). The emitter was operated at 1.9 kV. The mass spectra were measured in positive ion mode applying a top 20 data-dependent acquisition (DDA). The full MS was set to 70,000 resolution at m/z 200 [AGC target at 3e6, maximum injection time (IT) of 50 ms and a scan range 380-1800 (m/z)]. The full MS scan was followed by a MS/MS scan at 17,500 resolution at m/z 200 [Automatic Gain Control (AGC) target at 5e4, 1.2 m/z isolation window and maximum IT of 100 ms]. For MS/MS fragmentation, normalized collision energy (NCE) for higher energy collisional dissociation (HCD) was set to 27%. Dynamic exclusion was at 20 s. Unassigned and +1, +7, +8 and > +8 charged precursors were excluded. The intensity threshold was set to 1.0e4. The isotopes were excluded

Peptide and protein identification

Raw data were searched with the SEQUEST algorithm present in Proteome Discoverer version 1.3 (Thermo Scientific, Germany) described previously (Chaturvedi et al., 2015; Ghatak et al., 2020). Protein fasta employed was generated from the pan-transcriptome of three potato genotypes: Désirée, PW363 and Rywal (Petek et al., 2020). Peptides were matched against database plus decoys, considering a significant hit when the peptide confidence was high, which is equivalent to a false discovery rate (FDR) of 1%, and the Xcorr threshold was established at 1 per charge (2 for +2 ions 3 for +3 ions, etc.). The variable modifications were set to acetylation of

the N-terminus and methionine oxidation, with a mass tolerance of 10 ppm for the parent ion and 0.8 Da for the fragment ion. The number of missed and non-specific cleavages permitted was two. There were no fixed modifications, as dynamic modifications were used.

The MS/MS spectra of the identified proteins and their meta-information from both databases have been deposited to the ProteomeXchange Consortium via the PRIDE partner repository with the dataset identifier PXD052587. The identified proteins were quantitated based on total ion count and normalised using the normalised spectral abundance factor (NSAF) strategy (Paoletti et al., 2006).

Data analysis

Data preprocessing

Phenodata, a master sample description metadata file was constructed before sample collection (Supp. Table 1), according to FAIR principles. To detect any inconsistencies between replicates, pairwise plots between omics levels, multidimensional scaling plots and scatterplot matrices within omics' levels were constructed and examined using R v.4.3 (https://www.r-project.org/) and the package vegan v2.6-4 (Oksanen et al., 2022). Phenomics variable *deltaTemperature (*ΔT*)* was scaled by its minimal value to obtain nonnegative values for consecutive computing. Missing values in phenomics variable *water consumption* at day 1 were replaced by first day nonnegative values, i.e. measurements from day 3. Missing values in other omics' levels were imputed using random forest nonparametric missing value imputation approach (package missForest v1.5 (Stekhoven and Buhlmann, 2012)). Due to many missing values, the neoPA (hormonomics) variable was excluded from further analysis.

Variable selection was conducted on the non-invasive phenomics variable sets (Supp. Table 5). The random forest algorithms from the R package caret v6.0-94 (Kuhn, 2008) as well as the python package scikit-learn v1.2.0 were used with default settings, where recursive feature elimination was applied in R and mutual information was computed in Python v3.8, showing consistencies between the approaches for the top 5 variables (nonredundancy ranking in R). Sixth variable was selected by expert knowledge approach. Top area (normalised area of foreground pixels according to real-world coordinates), compactness (calculated as the ratio between area and surface of convex hull enveloping particular plan), qL_Lss (averaged intensity for steady-state fraction of open reaction centers in PSII in light), ΔT (averaged temperature of foreground pixels for steady-state temperature normalised to ambient temperature), water consumption, and

F_v/F_m_Lss (averaged intensity for maximum efficiency of PSII photochemistry in the light) were used in downstream analyses.

Gene set enrichment was performed on proteomics dataset using GSEA v4.3.2 application (Subramanian et al., 2005) and in-house generated gene set file (Supp. File 3, Supp. Table 4). Complete pipeline for proteomics differential expression was conducted using DEP v 1.22.0 package (Zhang et al., 2018) (Supp. Table 3). Sub-setting for downstream analyses was reasoned upon differential expression across various treatments combined with corresponding gene set annotations, i.e. pathways of utter importance for this experimental setup. Waterlogging stress was cut-off at one-week duration, while triple stress (Heat + Drought + Waterlogging) was not considered in downstream analyses due to poor plant performance.

Analysis of individual omics data layers

Pearson correlation coefficient (PCC) heatmaps (pheatmap v1.0.12, http://cran.nexr.com/web/packages/pheatmap/index.html; ComplexHeatmap v2.16.0) were generated within each treatment and for explicit treatment duration (Gu et al., 2016). Permutation-based t-test (MKinfer v1.1) was used to denote differences between specific treatment and control within the corresponding time-point (Kohl, 2024). To avoid ties, jitter was added to transcriptomics variables RD29B and SP6A in Heat condition at days 1, 7 and 8. Corresponding log2FC were calculated. For downstream analyses, 4 out of 6 replicates were chosen from non-invasive phenomics measurements to allow integration with invasive phenomics and other omics measurements conducted on 4 replicates.

Integration across different omics datasets

Correlations between components measured in various Omics' levels were calculated and visualised using DIABLO (Singh et al., 2019) as implemented in the mixOmics v6.24.0 package (Rohart et al., 2017). The correlation matrix was calculated separately for each stress as well as for control.

Integration of data with prior knowledge

A background knowledge network was manually constructed considering biochemical pathways between measured variables. Where necessary, pathways were simplified to only include representative variables, to prevent addition of many unmeasured nodes that would impede the visualisation. Proteomics differential expression results were merged with t-test and log2FC

results (Supp. Table 6) to inspect which parts of the network are responding in particular perturbation and visualised using DiNAR (Zagorscak et al., 2018) and Cytoscape (Shannon et al., 2003).

Experimentally acquired data and data required to reproduce the analysis are available from Supplemental Table 5 and NIB's GitHub repository.

Acknowledgements

The authors wish to thank Marijke Woudsma and Doretta Boomsma from HZPC Research for providing the Désirée plantlets for this study and Mirella Sorrentino for help with conducting the experiments at Photon Systems Instruments (PSI) Research Center (Drásov, Czech Republic). Moreover, we thank following colleagues for their assistance and expertise: S. Reid (FAU) and D. Pscheidt (FAU) for measuring metabolite content, and Katja Stare (NIB) and Nastja Marondini (NIB) for measuring gene expression.

Author contributions

KP, KG, SS, RS, CBa and MT conceptualized the study and designed the experiments, KP measured phenotypic traits, ŠB measured gene expression, ON, AP and JŠ measured hormone content, CS measured metabolite content, PC, AG prepared samples and performed proteomics analysis, LAS performed LC-MS measurements for proteomics analysis; MZ curated data; MZ, CB, AB, AZ and KG defined formal analysis methodology; MZ, CB, JZ, and AB conducted statistical, mathematical and computational analysis; MZ, LA, NR, CB, AB, ŠB and KG performed data visualisation; MZ, LA, NR, CB, SS, RS, KG, CBa and MT wrote the original draft. All authors edited the manuscript and approved the final manuscript version. Detailed author contributions are available from the Supp. Table 8.

Figure legends

Figure 1. Overview of the experimental design for single- and combined stress treatments and multi-omics sampling. A) Summary of cultivation conditions. Timeline of the experimental set-up and applied stress treatments, including the recovery phase in potato cv. Désirée. Timing and duration of stress treatment and days for tissue sampling are shown. (B) Actions comprised cultivation in the growing chambers and daily phenotyping with a set of sensors using the PlantScreen^{TM} phenotyping platform at PSI Research Center. (C) Automated image analysis pipeline was used to extract quantitative traits for morphological, physiological, and biochemical performance characterization of the plants during the stress treatment and recovery phase. Side view colour segmented RGB images of plants at selected time points

of tissue sampling (left panel) and daily plant volume (m^3) calculated from top and multiple angle side view RGB images (right panel). N=6.

Figure 2. Physiological profiling using high-throughput phenotyping platforms reveals distinct responses to single and combined stresses. A) Pixel-by-pixel false colour images of operating efficiency of photosystem II in light steady state (QY_Lss) captured by kinetic chlorophyll fluorescence measurement. Images for selected time points of tissue sampling are shown. Colour coding of the treatments apply for the entire figure. Vertical dashed lines indicate the onset and end of drought. B) QY_Lss values extracted from images for each individual time point. C) Steady-state fluorescence of maximum efficiency of PSII photochemistry in the light trait based on chlorophyll fluorescence top view (Fv/Fm_Lss). D) steady-state estimation of the fraction of open reaction centers in PSII trait in light based on chlorophyll fluorescence top view (qL_Lss). E) Difference between canopy average temperature extracted from thermal IR images and air temperature measured in the thermal IR imaging unit (ΔT). F) Water use efficiency (WUE) based on plant volume and water consumption. A-F) Black dotted lines reflect the initiation and removal of drought stress, respectively. G) Tuber numbers counted per plant on the last day of the experiment (Day 28 = 60 days of cultivation). H) Harvest index calculated from the total biomass and tuber weight on the last day of the experiment. G-H) Measurements, mean and standard deviation are shown (n = 4). Statistical evaluation of differences between groups is given by the non-parametric Kruskal–Wallis test (*one-way ANOVA on ranks*); p-value above x-axis, where asterisk denotes p-value < 0.05. See Figure 1A for scheme on stress treatments.

Figure 3: Integrated analysis of measured and generated data permits global visualization and multi-level amalgamation of potato stress responses. A) Schematics of tissue sampling protocol. 2^{nd} and 3^{rd} leaves were harvested for destructive “omics” analysis, 4^{th} leaf was used for relative water content calculation. Remaining plant tissue was quantified to obtain total above-ground biomass and tuber yield. B) Overview of data analysis pipeline. C) Dataset overview: multidimensional scaling shows combined HDW stressed plants as extremes, the centroid of each plant group is shown. D) Most informative variables from the phenomics level. Pearson correlation coefficients between them are presented as hierarchically clustered heat map in waterlogging and heat stress.

Figure 4: Integration of multi-omics data in a knowledge-based metabolic and signalling network. A) Structure of knowledge network. Individual studied components are coloured according to their function in different pathways. B) To compare the effects of different stresses on the overall state of the plant, we overlaid the knowledge networks with measured changes in component concentration. Nodes are coloured by log2 fold changes (red – increase in stress compared to control, blue – decrease in stress compared to control, grey – measurement not available) shown for two time points: sampling day 8 and sampling day 14 for the different stress treatments, days of stress treatment are given with each network (for more details of the set up see Figure 1A).

Figure 5: Combined heat and drought stress trigger distinct responses compared to each individual response. Additive effect of combined stress is most pronounced for branched chain amino acids accumulation and JA signalling response. A) Heatmaps showing log2FC (FDR p-value < 0.05) in individual stress heat (H) or drought (D) stress in comparison to combined one (HD) for targeted molecular analyses. Label colours indicate pathway associated with each molecule as in the Knowledge network (see Figure 4 for legend). B) Changes observed on proteomics level. Results of Gene Set Enrichment Analysis (FDR q-value < 0.1) are shown. For more information see Supp. Table 4. D) Biochemical knowledge network showing changes under combined HD stress at day 14 (treatment day 7). In this version of knowledge network, only nodes that were significantly differentially expressed (vs. control conditions) are coloured and the connections between two differentially expressed nodes are coloured black. Node full black border indicates molecules with higher expression levels in HD compared to H and/or D alone. Dashed black border indicates molecules with lower expression levels in HD compared to H and/or D alone (difference of log2FC > 0.5)**.**

Figure 6: Waterlogging triggers drought-stress like molecular responses in potato. A) Heatmaps showing log2FC (FDR p-value < 0.05) B) Volcano plot of differential proteomics analysis at day 7. Proteins with FDR p-value < 0.05 shown as blue (downregulated) and red (upregulated) dots. For more information see Supp. Table 3. C) Knowledge network of waterlogging stress at day 1 and day 7 (unfiltered, colour range [-2, 2]). For legend see Figure 4.

Figure 7. Schematic summary of multilevel responses to single and combined heat, drought and waterlogging stresses. Selected variables from each level are shown. Summary of molecular responses (hormones, metabolites and transcripts) was based on the comparisons illustrated in Figures 5 and 6. Summary of morphophysiological responses were based on the data from the last day of the experiment (Day 28), which includes tuber information. Proteomics data set is not included here due to the small dataset of differentially expressed proteins in the waterlogging treatment. Degree of increase or decrease is not specified.

Supplementary data

Supplementary File 1: Principal coordinates analysis (PCoA) of Bray-Curtis dissimilarity between samples. Interactive 3D plot shows mapping to three dimensions. Spheres are coloured by condition. The numerical values used to construct this figure can be found in Supplementary Table 5. Variables were min-max scaled.

Supplementary File 2: Differential Network Analysis animation. Export from DiNAR app (Zagorščak et al., 2018). Node colours correspond to upregulation (red) and downregulation (blue) compared to

control (p-value adjusted < 0.05). The size of nodes corresponds to absolute log2FC values. Order of visualisation: 0: background network, 1: 1 day of drought, 2: one week of drought 3: one day of heat, 4: one week of heat, 5: 8 days of heat, 6: two weeks of heat, 7: 8 days of heat + one day of drought, 8: two weeks of heat + one week of drought, 9: one day of waterlogging, 10: one week of waterlogging.

Supplementary File 3: Pan-transcriptome Gene Matrix Transposed (GMT) file format. Tab delimited file utilised for gene set enrichment analysis that describes gene sets from pan-transcriptome of three potato genotypes: Désirée, PW363 and Rywal (Petek et al., 2020).

Supplementary Figure 1: Plant morphological responses of control and stress-treated plants. (A) Top view RGB images at selected time points of tissue sampling starting from day 1 where i) in the first week heat stress was induced for H, HD, HDW marked rows, then ii) in the second week drought was induced for D, HD, HDW up to day 14, and finally iii) in the third week waterlogging was induced for HDW up to day 21, while the other treatments were recovered. (B-E) Parameters based on analysed RGB images; Top area, plant height, compactness, and relative growth rate (RGR). The data represent mean values ± standard error of mean (S.E.M) (n = 6).

Supplementary Figure 2: Log2FC of a tuber metabolite's relative abundance between stress and control. Numbers in bold correspond to comparisons with p-value < 0.05. Additionally, log2FC for number of tubers and total tuber weight is shown.

Supplementary Figure 3: Correlation analysis within and between omics levels. For correlation analysis within omics levels heatmaps display Pearson correlation coefficient (PCC). For analysis between components of different molecular levels heatmaps display canonical correlation analysis (CCA) results. Variable prioritisation was conducted using multiblock sPLS-DA (Singh et al., 2019).

Supplementary Table 1: Phenodata. Experimental design and days of tissue sampling.

Supplementary Table 2: Phenomics featuredata. Phenotyping trait description from multiple imaging sensors and traits from the final destructive harvest.

Supplementary Table 3: Differential protein expression. Results table of differential protein expression from R package DEP (Zhang et al., 2018) complemented by MapMan annotations (Ramšak et al., 2014) and Arabidopsis thaliana orthologue identifiers, short names, and gene descriptions (Bleker at al., 2024, Zagorščak et al., 2018).

Supplementary Table 4: Gene set enrichment analysis of proteomics data. MapMan v3 pathway enrichment results containing classes of proteins that are over-represented in stress treatments compared to control (FDR cut-off 0.05 and 0.1). MapMan pathways are defined in supplementary file 3.

Supplementary Table 5: Omics measurements. Multi-sheet file containing tuber (metabolomics, harvest information) and leaf data (phenomics, transcriptomics, hormonomics and metabolomics). Phenomics data is separated to non-invasive and invasive trait measurements. For trait description see Supplementary Table 2.

Supplementary Table 6: Statistical results across different omics levels. Combined table contains statistical information and various annotations for molecules shown in biochemical knowledge network (see Figure 4,5,6 and Supplementary File 2).

Supplementary Table 7: Genes used for transcriptome analysis using quantitative PCR. Gene functional group, name (abbreviation) and description, as well as corresponding primer and probe sequences, source and amplification efficiency are shown. Suitability of reference genes was validated using RefFinder (Xie et al., 2023).

Supplementary Table 8: CRediT (Contributor Roles Taxonomy) authorship statement.

Competing interests

The authors declare no competing interests.

Funding

This work was funded by the EU H2020-SFS-2019-2 RIA project ADAPT, GA 2020 862-858, Aris P4-0165, J2-3060 and Z4-50146. Moreover, this work was partially supported by the Ministry of Education, Youth and Sports of the Czech Republic with the European Regional Development Fund-Project “SINGING PLANT” (no. CZ.02.1.01/0.0/0.0/16_026/0008446).

Data availability statement

Experimentally acquired data and data required to reproduce the analysis are available from Supp. Table 5 and NIBs' GitHub repository https://github.com/NIB-SI/multiOmics-integration. Proteomics data are available via ProteomeXchange with identifier PXD052587.

References

Abdelhakim LOA, Rosenqvist E, Wollenweber B, Spyroglou I, Ottosen C-O, Panzarová K (2021) Investigating Combined Drought- and Heat Stress Effects in Wheat under Controlled Conditions by Dynamic Image-Based Phenotyping. Agronomy **11:** 364

Abelenda JA, Bergonzi S, Oortwijn M, Sonnewald S, Du M, Visser RGF, Sonnewald U, Bachem CWB (2019) Source-Sink Regulation Is Mediated by Interaction of an FT Homolog with a SWEET Protein in Potato. Curr Biol **29:** 1178-1186 e1176

Abelenda JA, Cruz-Oro E, Franco-Zorrilla JM, Prat S (2016) Potato StCONSTANS-like1 Suppresses Storage Organ Formation by Directly Activating the FT-like StSP5G Repressor. Curr Biol **26:** 872-881

Akbudak MA, Yildiz S, Filiz E (2020) Pathogenesis related protein-1 (PR-1) genes in tomato (Solanum lycopersicum L.): Bioinformatics analyses and expression profiles in response to drought stress. Genomics **112:** 4089-4099

Awlia M, Nigro A, Fajkus J, Schmoeckel SM, Negrao S, Santelia D, Trtilek M, Tester M, Julkowska MM, Panzarova K (2016) High-Throughput Non-destructive Phenotyping of Traits that Contribute to Salinity Tolerance in Arabidopsis thaliana. Front Plant Sci **7:** 1414

Bachmann A, Hause B, Maucher H, Garbe E, Voros K, Weichert H, Wasternack C, Feussner I (2002) Jasmonate-induced lipid peroxidation in barley leaves initiated by distinct 13-LOX forms of chloroplasts. Biol Chem **383:** 1645-1657

Baebler S, Svalina M, Petek M, Stare K, Rotter A, Pompe-Novak M, Gruden K (2017) quantGenius: implementation of a decision support system for qPCR-based gene quantification. BMC Bioinformatics **18:** 276

Bailey-Serres J, Parker JE, Ainsworth EA, Oldroyd GED, Schroeder JI (2019) Genetic strategies for improving crop yields. Nature **575:** 109-118

Balfagon D, Sengupta S, Gomez-Cadenas A, Fritschi FB, Azad RK, Mittler R, Zandalinas SI (2019) Jasmonic Acid Is Required for Plant Acclimation to a Combination of High Light and Heat Stress. Plant Physiol **181:** 1668-1682

Benitez-Alfonso Y, Soanes BK, Zimba S, Sinanaj B, German L, Sharma V, Bohra A, Kolesnikova A, Dunn JA, Martin AC, Khashi URM, Saati-Santamaria Z, Garcia-Fraile P, Ferreira EA, Frazao LA, Cowling WA, Siddique KHM, Pandey MK, Farooq M, Varshney RK, Chapman MA, Boesch C, Daszkowska-Golec A, Foyer CH (2023) Enhancing climate change resilience in agricultural crops. Curr Biol **33:** R1246-R1261

Bittner A, Ciesla A, Gruden K, Lukan T, Mahmud S, Teige M, Vothknecht UC, Wurzinger B (2022) Organelles and phytohormones: a network of interactions in plant stress responses. J Exp Bot **73:** 7165-7181

Bleker C, Ramsak Z, Bittner A, Podpecan V, Zagorscak M, Wurzinger B, Baebler S, Petek M, Kriznik M, van Dieren A, Gruber J, Afjehi-Sadat L, Weckwerth W, Zupanic A, Teige M, Vothknecht UC, Gruden K (2024) Stress Knowledge Map: A knowledge graph resource for systems biology analysis of plant stress responses. Plant Commun**:** 100920

Bradshaw JE, Hackett CA, Pande B, Waugh R, Bryan GJ (2008) QTL mapping of yield, agronomic and quality traits in tetraploid potato (Solanum tuberosum subsp. tuberosum). Theor Appl Genet **116:** 193-211

Chaturvedi P, Doerfler H, Jegadeesan S, Ghatak A, Pressman E, Castillejo MA, Wienkoop S, Egelhofer V, Firon N, Weckwerth W (2015) Heat-Treatment-Responsive Proteins in Different Developmental Stages of Tomato Pollen Detected by Targeted Mass Accuracy Precursor Alignment (tMAPA). J Proteome Res **14:** 4463-4471

Chaturvedi P, Ischebeck T, Egelhofer V, Lichtscheidl I, Weckwerth W (2013) Cell-specific analysis of the tomato pollen proteome from pollen mother cell to mature pollen provides evidence for developmental priming. J Proteome Res **12:** 4892-4903

Clarke SM, Cristescu SM, Miersch O, Harren FJM, Wasternack C, Mur LAJ (2009) Jasmonates act with salicylic acid to confer basal thermotolerance in Arabidopsis thaliana. New Phytol **182:** 175-187

Cutler SR, Rodriguez PL, Finkelstein RR, Abrams SR (2010) Abscisic acid: emergence of a core signaling network. Annu Rev Plant Biol **61:** 651-679

Dahal K, Li XQ, Tai H, Creelman A, Bizimungu B (2019) Improving Potato Stress Tolerance and Tuber Yield Under a Climate Change Scenario - A Current Overview. Front Plant Sci **10:** 563

Demirel U, Morris WL, Ducreux LJM, Yavuz C, Asim A, Tindas I, Campbell R, Morris JA, Verrall SR, Hedley PE, Gokce ZNO, Caliskan S, Aksoy E, Caliskan ME, Taylor MA,

Hancock RD (2020) Physiological, Biochemical, and Transcriptional Responses to Single and Combined Abiotic Stress in Stress-Tolerant and Stress-Sensitive Potato Genotypes. Front Plant Sci **11:** 169

FAO (2023) The Impact of Disasters on Agriculture and Food Security 2023 – Avoiding and reducing losses through investment in resilience. . *In*. FAO, Rome, Italy, p #168 p.

Findurová H, Veselá B, Panzarová K, Pytela J, Trtílek M, Klem K (2023) Phenotyping drought tolerance and yield performance of barley using a combination of imaging methods. Environmental and Experimental Botany **209:** 105314

Flokova K, Tarkowska D, Miersch O, Strnad M, Wasternack C, Novak O (2014) UHPLC-MS/MS based target profiling of stress-induced phytohormones. Phytochemistry **105:** 147-157

Geldhof B, Pattyn J, Van de Poel B (2023) From a different angle: genetic diversity underlies differentiation of waterlogging-induced epinasty in tomato. Front Plant Sci **14:** 1178778

George TS, Taylor MA, Dodd IC, White PJ (2017) Climate Change and Consequences for Potato Production: a Review of Tolerance to Emerging Abiotic Stress. Potato Research **60:** 239-268

Ghatak A, Chaturvedi P, Bachmann G, Valledor L, Ramsak Z, Bazargani MM, Bajaj P, Jegadeesan S, Li W, Sun X, Gruden K, Varshney RK, Weckwerth W (2020) Physiological and Proteomic Signatures Reveal Mechanisms of Superior Drought Resilience in Pearl Millet Compared to Wheat. Front Plant Sci **11:** 600278

Ghatak A, Chaturvedi P, Nagler M, Roustan V, Lyon D, Bachmann G, Postl W, Schrofl A, Desai N, Varshney RK, Weckwerth W (2016) Comprehensive tissue-specific proteome analysis of drought stress responses in Pennisetum glaucum (L.) R. Br. (Pearl millet). J Proteomics **143:** 122-135

Grieco M, Roustan V, Dermendjiev G, Rantala S, Jain A, Leonardelli M, Neumann K, Berger V, Engelmeier D, Bachmann G, Ebersberger I, Aro EM, Weckwerth W, Teige M (2020) Adjustment of photosynthetic activity to drought and fluctuating light in wheat. Plant Cell Environ **43:** 1484-1500

Gu Z, Eils R, Schlesner M (2016) Complex heatmaps reveal patterns and correlations in multidimensional genomic data. Bioinformatics **32:** 2847-2849

Guihur A, Rebeaud ME, Goloubinoff P (2022) How do plants feel the heat and survive? Trends Biochem Sci **47:** 824-838

Hall RD, D'Auria JC, Silva Ferreira AC, Gibon Y, Kruszka D, Mishra P, van de Zedde R (2022) High-throughput plant phenotyping: a role for metabolomics? Trends Plant Sci **27:** 549-563

Hancock RD, Morris WL, Ducreux LJ, Morris JA, Usman M, Verrall SR, Fuller J, Simpson CG, Zhang R, Hedley PE, Taylor MA (2014) Physiological, biochemical and molecular responses of the potato (Solanum tuberosum L.) plant to moderately elevated temperature. Plant Cell Environ **37:** 439-450

Hastilestari BR, Lorenz J, Reid S, Hofmann J, Pscheidt D, Sonnewald U, Sonnewald S (2018) Deciphering source and sink responses of potato plants (Solanum tuberosum L.) to elevated temperatures. Plant Cell Environ **41:** 2600-2616

Hoehenwarter W, van Dongen JT, Wienkoop S, Steinfath M, Hummel J, Erban A, Sulpice R, Regierer B, Kopka J, Geigenberger P, Weckwerth W (2008) A rapid approach for phenotype-screening and database independent detection of cSNP/protein polymorphism using mass accuracy precursor alignment. Proteomics **8:** 4214-4225

Hoopes G, Meng X, Hamilton JP, Achakkagari SR, de Alves Freitas Guesdes F, Bolger ME, Coombs JJ, Esselink D, Kaiser NR, Kodde L, Kyriakidou M, Lavrijssen B, van Lieshout N, Shereda R, Tuttle HK, Vaillancourt B, Wood JC, de Boer JM, Bornowski N, Bourke P, Douches D, van Eck HJ, Ellis D, Feldman MJ, Gardner KM, Hopman JCP, Jiang J, De Jong WS, Kuhl JC, Novy RG, Oome S, Sathuvalli V, Tan

EH, Ursum RA, Vales MI, Vining K, Visser RGF, Vossen J, Yencho GC, Anglin NL, Bachem CWB, Endelman JB, Shannon LM, Stromvik MV, Tai HH, Usadel B, Buell CR, Finkers R (2022) Phased, chromosome-scale genome assemblies of tetraploid potato reveal a complex genome, transcriptome, and predicted proteome landscape underpinning genetic diversity. Mol Plant **15:** 520-536

JACKSON MB, CAMPBELL DJ (1976) WATERLOGGING AND PETIOLE EPINASTY IN TOMATO: THE ROLE OF ETHYLENE AND LOW OXYGEN. New Phytologist **76:** 21-29

JACKSON MB, HALL KC (1987) Early stomatal closure in waterlogged pea plants is mediated by abscisic acid in the absence of foliar water deficits. Plant, Cell & Environment **10:** 121-130

Jamil IN, Remali J, Azizan KA, Nor Muhammad NA, Arita M, Goh HH, Aizat WM (2020) Systematic Multi-Omics Integration (MOI) Approach in Plant Systems Biology. Front Plant Sci **11:** 944

Joshi S, Patil S, Shaikh A, Jamla M, Kumar V (2024) Modern omics toolbox for producing combined and multifactorial abiotic stress tolerant plants. Plant Stress **11:** 100301

Jovović Z, Broćić A, Velimirović ŽD, A. Komnenić (2021) The influence of flooding on the main parameters of potato productivity. *In*, Ed 1320. International Society for Horticultural Science (ISHS), Leuven, Belgium, pp 133-138

Kanehisa M, Furumichi M, Tanabe M, Sato Y, Morishima K (2017) KEGG: new perspectives on genomes, pathways, diseases and drugs. Nucleic Acids Res **45:** D353-D361

Kloosterman B, Abelenda JA, Gomez Mdel M, Oortwijn M, de Boer JM, Kowitwanich K, Horvath BM, van Eck HJ, Smaczniak C, Prat S, Visser RG, Bachem CW (2013) Naturally occurring allele diversity allows potato cultivation in northern latitudes. Nature **495:** 246-250

Klukas C, Chen D, Pape JM (2014) Integrated Analysis Platform: An Open-Source Information System for High-Throughput Plant Phenotyping. Plant Physiol **165:** 506-518

Koch L, Lehretz GG, Sonnewald U, Sonnewald S (2024) Yield reduction caused by elevated temperatures and high nitrogen fertilization is mitigated by SP6A overexpression in potato (Solanum tuberosum L.). Plant J **117:** 1702-1715

Kohl M (2024) MKinfer: Inferential Statistics. R package **Version 1.2:** https://github.com/stamats/MKinfer

Kromdijk J, Glowacka K, Leonelli L, Gabilly ST, Iwai M, Niyogi KK, Long SP (2016) Improving photosynthesis and crop productivity by accelerating recovery from photoprotection. Science **354:** 857-861

Kuhn M (2008) Building Predictive Models in R Using the caret Package. Journal of Statistical Software **28:** 1 - 26

Lal MK, Tiwari RK, Kumar A, Dey A, Kumar R, Kumar D, Jaiswal A, Changan SS, Raigond P, Dutt S, Luthra SK, Mandal S, Singh MP, Paul V, Singh B (2022) Mechanistic Concept of Physiological, Biochemical, and Molecular Responses of the Potato Crop to Heat and Drought Stress. Plants (Basel) **11**

Lee AH, Shannon CP, Amenyogbe N, Bennike TB, Diray-Arce J, Idoko OT, Gill EE, Ben-Othman R, Pomat WS, van Haren SD, Cao KL, Cox M, Darboe A, Falsafi R, Ferrari D, Harbeson DJ, He D, Bing C, Hinshaw SJ, Ndure J, Njie-Jobe J, Pettengill MA, Richmond PC, Ford R, Saleu G, Masiria G, Matlam JP, Kirarock W, Roberts E, Malek M, Sanchez-Schmitz G, Singh A, Angelidou A, Smolen KK, Consortium E, Brinkman RR, Ozonoff A, Hancock REW, van den Biggelaar AHJ, Steen H, Tebbutt SJ, Kampmann B, Levy O, Kollmann TR (2019) Dynamic molecular changes during the first week of human life follow a robust developmental trajectory. Nat Commun **10:** 1092

Leeggangers HACF, Rodriguez-Granados NY, Macias-Honti MG, Sasidharan R (2023) A helping hand when drowning: The versatile role of ethylene in root flooding resilience. Environmental and Experimental Botany **213:** 105422

Lehretz GG, Sonnewald S, Lugassi N, Granot D, Sonnewald U (2020) Future-Proofing Potato for Drought and Heat Tolerance by Overexpression of Hexokinase and SP6A. Front Plant Sci **11:** 614534

Leisner CP, Hamilton JP, Crisovan E, Manrique-Carpintero NC, Marand AP, Newton L, Pham GM, Jiang J, Douches DS, Jansky SH, Buell CR (2018) Genome sequence of M6, a diploid inbred clone of the high-glycoalkaloid-producing tuber-bearing potato species Solanum chacoense, reveals residual heterozygosity. Plant J **94:** 562-570

Li B, Zeng Y, Cao W, Zhang W, Cheng L, Yin H, Wu Q, Wang X, Huang Y, Lau WCY, Yao ZP, Guo Y, Jiang L (2021) A distinct giant coat protein complex II vesicle population in Arabidopsis thaliana. Nat Plants **7:** 1335-1346

Liu K, Harrison MT, Yan H, Liu L, Meinke H, Hoogenboom G, Wang B, Peng B, Guan K, Jaegermeyr J, Wang E, Zhang F, Yin X, Archontoulis S, Nie L, Badea A, Man J, Wallach D, Zhao J, Benjumea AB, Fahad S, Tian X, Wang W, Tao F, Zhang Z, Rotter R, Yuan Y, Zhu M, Dai P, Nie J, Yang Y, Zhang Y, Zhou M (2023) Silver lining to a climate crisis in multiple prospects for alleviating crop waterlogging under future climates. Nat Commun **14:** 765

Liu T, Salguero P, Petek M, Martinez-Mira C, Balzano-Nogueira L, Ramsak Z, McIntyre L, Gruden K, Tarazona S, Conesa A (2022) PaintOmics 4: new tools for the integrative analysis of multi-omics datasets supported by multiple pathway databases. Nucleic Acids Res **50:** W551-W559

Lozano-Elena F, Fàbregas N, Coleto-Alcudia V, Caño-Delgado AI (2022) Analysis of metabolic dynamics during drought stress in Arabidopsis plants. Scientific Data **9:** 90

Lozano-Juste J, Cutler SR (2016) Hormone signalling: ABA has a breakdown. Nat Plants **2:** 16137

Mahmud S, Ullah C, Kortz A, Bhattacharyya S, Yu P, Gershenzon J, Vothknecht UC (2022) Constitutive expression of JASMONATE RESISTANT 1 induces molecular changes that prime the plants to better withstand drought. Plant Cell Environ **45:** 2906-2922

Manjunath KK, Krishna H, Devate NB, Sunilkumar VP, Patil SP, Chauhan D, Singh S, Kumar S, Jain N, Singh GP, Singh PK (2023) QTL mapping: insights into genomic regions governing component traits of yield under combined heat and drought stress in wheat. Front Genet **14:** 1282240

Mathur S, Agrawal D, Jajoo A (2014) Photosynthesis: Response to high temperature stress. Journal of Photochemistry and Photobiology B: Biology **137:** 116-126

Mishra S, Srivastava AK, Khan AW, Tran LP, Nguyen HT (2024) The era of panomics-driven gene discovery in plants. Trends Plant Sci

Mittler R (2006) Abiotic stress, the field environment and stress combination. Trends Plant Sci **11:** 15-19

Nakamura Y, Mithofer A, Kombrink E, Boland W, Hamamoto S, Uozumi N, Tohma K, Ueda M (2011) 12-hydroxyjasmonic acid glucoside is a COI1-JAZ-independent activator of leaf-closing movement in Samanea saman. Plant Physiol **155:** 1226-1236

Navarro C, Abelenda JA, Cruz-Oro E, Cuellar CA, Tamaki S, Silva J, Shimamoto K, Prat S (2011) Control of flowering and storage organ formation in potato by FLOWERING LOCUS T. Nature **478:** 119-122

Núñez-Lillo G, Ponce E, Arancibia-Guerra C, Carpentier S, Carrasco-Pancorbo A, Olmo-García L, Chirinos R, Campos D, Campos-Vargas R, Meneses C, Pedreschi R (2023) A multiomics integrative analysis of color de-synchronization with softening of 'Hass' avocado fruit: A first insight into a complex physiological disorder. Food Chemistry **408:** 135215

Núñez-Lillo G, Ponce E, Beyer CP, Álvaro JE, Meneses C, Pedreschi R (2024) A First Omics Data Integration Approach in Hass Avocados to Evaluate Rootstock–Scion Interactions: From Aerial and Root Plant Growth to Fruit Development. Plants **13:** 603

Obata T, Klemens PAW, Rosado-Souza L, Schlereth A, Gisel A, Stavolone L, Zierer W, Morales N, Mueller LA, Zeeman SC, Ludewig F, Stitt M, Sonnewald U, Neuhaus HE, Fernie AR (2020) Metabolic profiles of six African cultivars of cassava (Manihot esculenta Crantz) highlight bottlenecks of root yield. Plant J **102:** 1202-1219

Oksanen J, Simpson G, Blanchet FG, Kindt R, Legendre P, Minchin P, hara R, Solymos P, Stevens H, Szöcs E, Wagner H, Barbour M, Bedward M, Bolker B, Borcard D, Carvalho G, Chirico M, De Cáceres M, Durand S, Weedon J (2022) vegan community ecology package version 2.6-2 April 2022,

Paoletti AC, Parmely TJ, Tomomori-Sato C, Sato S, Zhu D, Conaway RC, Conaway JW, Florens L, Washburn MP (2006) Quantitative proteomic analysis of distinct mammalian Mediator complexes using normalized spectral abundance factors. Proc Natl Acad Sci U S A **103:** 18928-18933

Park JS, Park SJ, Kwon SY, Shin AY, Moon KB, Park JM, Cho HS, Park SU, Jeon JH, Kim HS, Lee HJ (2022) Temporally distinct regulatory pathways coordinate thermo-responsive storage organ formation in potato. Cell Rep **38:** 110579

Paul K, Sorrentino M, Lucini L, Rouphael Y, Cardarelli M, Bonini P, Reynaud H, Canaguier R, Trtilek M, Panzarova K, Colla G (2019) Understanding the Biostimulant Action of Vegetal-Derived Protein Hydrolysates by High-Throughput Plant Phenotyping and Metabolomics: A Case Study on Tomato. Front Plant Sci **10:** 47

Petek M, Rotter A, Kogovsek P, Baebler S, Mithofer A, Gruden K (2014) Potato virus Y infection hinders potato defence response and renders plants more vulnerable to Colorado potato beetle attack. Mol Ecol **23:** 5378-5391

Petek M, Zagorscak M, Ramsak Z, Sanders S, Tomaz S, Tseng E, Zouine M, Coll A, Gruden K (2020) Cultivar-specific transcriptome and pan-transcriptome reconstruction of tetraploid potato. Sci Data **7:** 249

Pham GM, Hamilton JP, Wood JC, Burke JT, Zhao H, Vaillancourt B, Ou S, Jiang J, Buell CR (2020) Construction of a chromosome-scale long-read reference genome assembly for potato. Gigascience **9**

Ployet R, Veneziano Labate MT, Regiani Cataldi T, Christina M, Morel M, San Clemente H, Denis M, Favreau B, Tomazello Filho M, Laclau J-P, Labate CA, Chaix G, Grima-Pettenati J, Mounet F (2019) A systems biology view of wood formation in Eucalyptus grandis trees submitted to different potassium and water regimes. New Phytologist **223:** 766-782

Quint M, Delker C, Franklin KA, Wigge PA, Halliday KJ, van Zanten M (2016) Molecular and genetic control of plant thermomorphogenesis. Nat Plants **2:** 15190

Renziehausen T, Frings S, Schmidt-Schippers R (2024) 'Against all floods': plant adaptation to flooding stress and combined abiotic stresses. Plant J

Rivero RM, Mittler R, Blumwald E, Zandalinas SI (2022) Developing climate-resilient crops: improving plant tolerance to stress combination. Plant J **109:** 373-389

Rohart F, Gautier B, Singh A, Le Cao KA (2017) mixOmics: An R package for 'omics feature selection and multiple data integration. PLoS Comput Biol **13:** e1005752

Sato H, Mizoi J, Shinozaki K, Yamaguchi-Shinozaki K (2024) Complex plant responses to drought and heat stress under climate change. Plant J

Sauter M (2013) Root responses to flooding. Curr Opin Plant Biol **16:** 282-286

Shannon P, Markiel A, Ozier O, Baliga NS, Wang JT, Ramage D, Amin N, Schwikowski B, Ideker T (2003) Cytoscape: a software environment for integrated models of biomolecular interaction networks. Genome Res **13:** 2498-2504

Singh A, Shannon CP, Gautier B, Rohart F, Vacher M, Tebbutt SJ, Lê Cao K-A (2019) DIABLO: an integrative approach for identifying key molecular drivers from multi-omics assays. Bioinformatics **35:** 3055-3062

Sinha R, Pelaez-Vico MA, Shostak B, Nguyen TT, Pascual LS, Ogden AM, Lyu Z, Zandalinas SI, Joshi T, Fritschi FB, Mittler R (2024) The effects of multifactorial stress combination on rice and maize. Plant Physiol **194:** 1358-1369

Siroka J, Brunoni F, Pencik A, Mik V, Zukauskaite A, Strnad M, Novak O, Flokova K (2022) High-throughput interspecies profiling of acidic plant hormones using miniaturised sample processing. Plant Methods **18:** 122

Smith AM, Zeeman SC (2006) Quantification of starch in plant tissues. Nat Protoc **1:** 1342-1345

Stael S, Kmiecik P, Willems P, Van Der Kelen K, Coll NS, Teige M, Van Breusegem F (2015) Plant innate immunity--sunny side up? Trends Plant Sci **20:** 3-11

Stekhoven DJ, Buhlmann P (2012) MissForest--non-parametric missing value imputation for mixed-type data. Bioinformatics **28:** 112-118

Subramanian A, Tamayo P, Mootha VK, Mukherjee S, Ebert BL, Gillette MA, Paulovich A, Pomeroy SL, Golub TR, Lander ES, Mesirov JP (2005) Gene set enrichment analysis: a knowledge-based approach for interpreting genome-wide expression profiles. Proc Natl Acad Sci U S A **102:** 15545-15550

Tang D, Jia Y, Zhang J, Li H, Cheng L, Wang P, Bao Z, Liu Z, Feng S, Zhu X, Li D, Zhu G, Wang H, Zhou Y, Zhou Y, Bryan GJ, Buell CR, Zhang C, Huang S (2022) Genome evolution and diversity of wild and cultivated potatoes. Nature **606:** 535-541

Tang R, Niu S, Zhang G, Chen G, Haroon M, Yang Q, Rajora OP, Li X-Q (2018) Physiological and growth responses of potato cultivars to heat stress. Botany **96:** 897-912

Trapero-Mozos A, Morris WL, Ducreux LJM, McLean K, Stephens J, Torrance L, Bryan GJ, Hancock RD, Taylor MA (2018) Engineering heat tolerance in potato by temperature-dependent expression of a specific allele of HEAT-SHOCK COGNATE 70. Plant Biotechnol J **16:** 197-207

von Gehren P, Bomers S, Tripolt T, Söllinger J, Prat N, Redondo B, Vorss R, Teige M, Kamptner A, Ribarits A (2023) Farmers Feel the Climate Change: Variety Choice as an Adaptation Strategy of European Potato Farmers. Climate **11:** 189

Wasternack C, Feussner I (2018) The Oxylipin Pathways: Biochemistry and Function. Annu Rev Plant Biol **69:** 363-386

Weckwerth W, Ghatak A, Bellaire A, Chaturvedi P, Varshney RK (2020) PANOMICS meets germplasm. Plant Biotechnol J **18:** 1507-1525

Weng JK, Ye M, Li B, Noel JP (2016) Co-evolution of Hormone Metabolism and Signaling Networks Expands Plant Adaptive Plasticity. Cell **166:** 881-893

Wu Q, Su N, Huang X, Cui J, Shabala L, Zhou M, Yu M, Shabala S (2021) Hypoxia-induced increase in GABA content is essential for restoration of membrane potential and preventing ROS-induced disturbance to ion homeostasis. Plant Commun **2:** 100188

Yang W, Feng H, Zhang X, Zhang J, Doonan JH, Batchelor WD, Xiong L, Yan J (2020) Crop Phenomics and High-Throughput Phenotyping: Past Decades, Current Challenges, and Future Perspectives. Mol Plant **13:** 187-214

Yoshida T, Fernie AR (2024) Hormonal regulation of plant primary metabolism under drought. J Exp Bot **75:** 1714-1725

Yoshihara T, Omir E-SA, Koshino H, Sakamura S, Kkuta Y, Koda Y (1989) Structure of a Tuber-inducing Stimulus from Potato Leaves (Solanum tuberosum L.). Agricultural and Biological Chemistry **53:** 2835-2837

Zagorscak M, Blejec A, Ramsak Z, Petek M, Stare T, Gruden K (2018) DiNAR: revealing hidden patterns of plant signalling dynamics using Differential Network Analysis in R. Plant Methods **14:** 78

Zaki HEM, Radwan KSA (2022) Response of potato (Solanum tuberosum L.) cultivars to drought stress under in vitro and field conditions. Chemical and Biological Technologies in Agriculture **9:** 1

Zandalinas SI, Fritschi FB, Mittler R (2021) Global Warming, Climate Change, and Environmental Pollution: Recipe for a Multifactorial Stress Combination Disaster. Trends Plant Sci **26:** 588-599

Zandalinas SI, Pelaez-Vico MA, Sinha R, Pascual LS, Mittler R (2023) The impact of multifactorial stress combination on plants, crops, and ecosystems: how should we prepare for what comes next? Plant J

Zeng ZL, Wang XQ, Zhang SB, Huang W (2024) Mesophyll conductance limits photosynthesis in fluctuating light under combined drought and heat stresses. Plant Physiol **194:** 1498-1511

Zhang H, Sonnewald U (2017) Differences and commonalities of plant responses to single and combined stresses. Plant J **90:** 839-855

Zhang H, Zhu J, Gong Z, Zhu JK (2022) Abiotic stress responses in plants. Nat Rev Genet **23:** 104-119

Zhang R, Zhang C, Yu C, Dong J, Hu J (2022) Integration of multi-omics technologies for crop improvement: Status and prospects. Front Bioinform **2:** 1027457

Zhang X, Smits AH, van Tilburg GB, Ovaa H, Huber W, Vermeulen M (2018) Proteome-wide identification of ubiquitin interactions using UbIA-MS. Nat Protoc **13:** 530-550

Zhao Y, Zhang W, Abou-Elwafa SF, Shabala S, Xu L (2021) Understanding a Mechanistic Basis of ABA Involvement in Plant Adaptation to Soil Flooding: The Current Standing. Plants (Basel) **10**